CR PROPAGATION IN THE GALAXY: INSIGHTS FROM TeV HALOS, THE DIFFUSE γ-RAY EMISSION, AND THE CR ANISOTROPY

Gwenael Giacinti
(APC Paris, CNRS)

Collaborators include Yiwei Bao, Samy Kaci, and Yuan Li

Cosmic-rays & their secondaries :

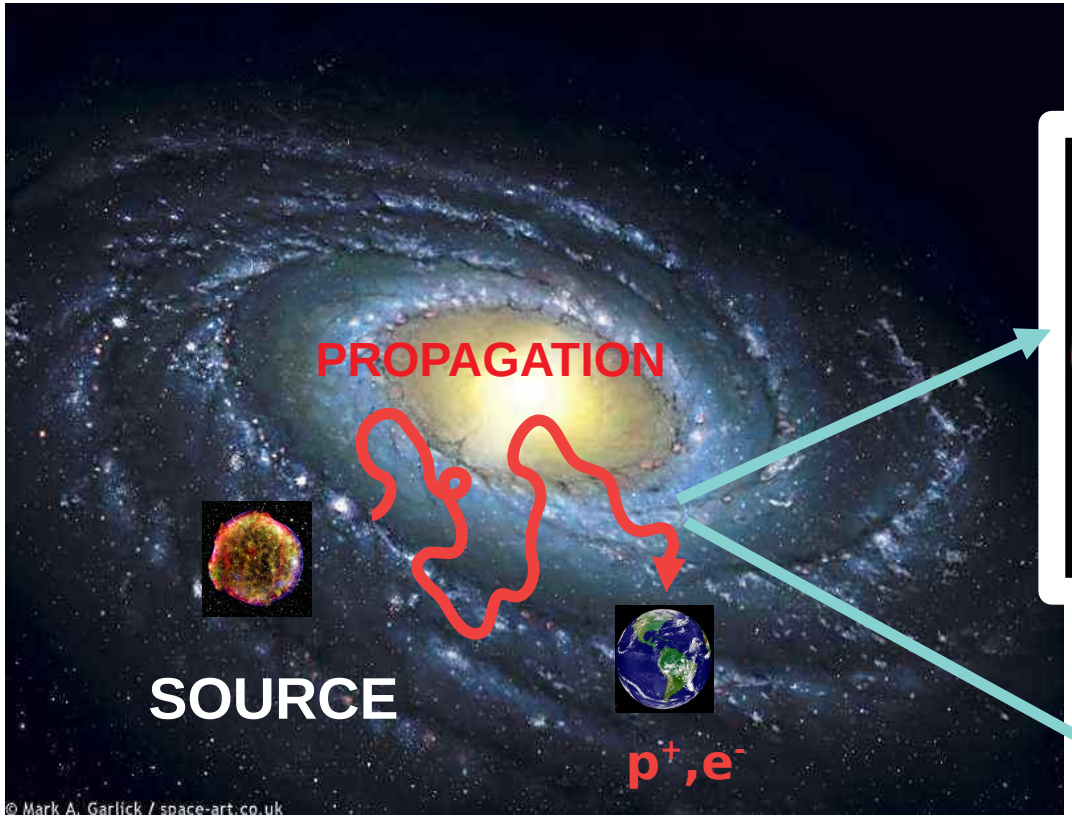

Produce γ-rays, neutrinos:

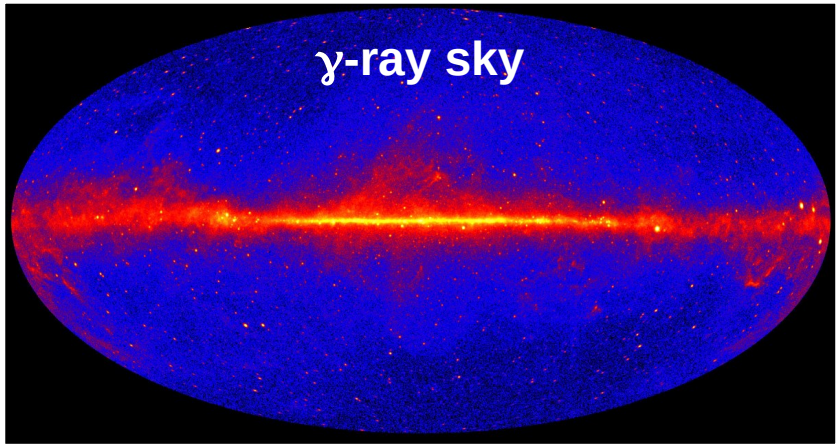

ν sky

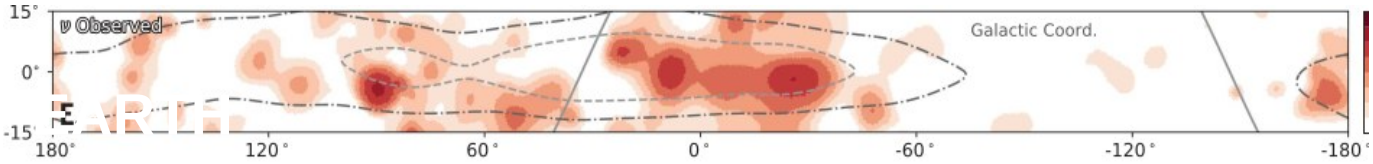

Simplified Milky Way seen edge-on :

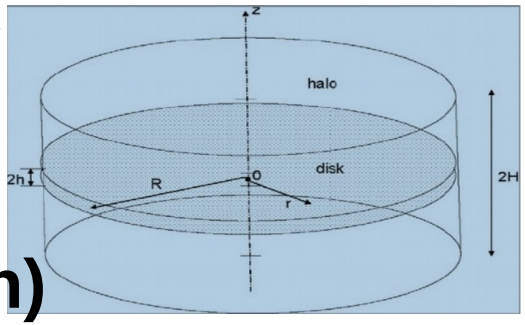

(if iso. diffusion)

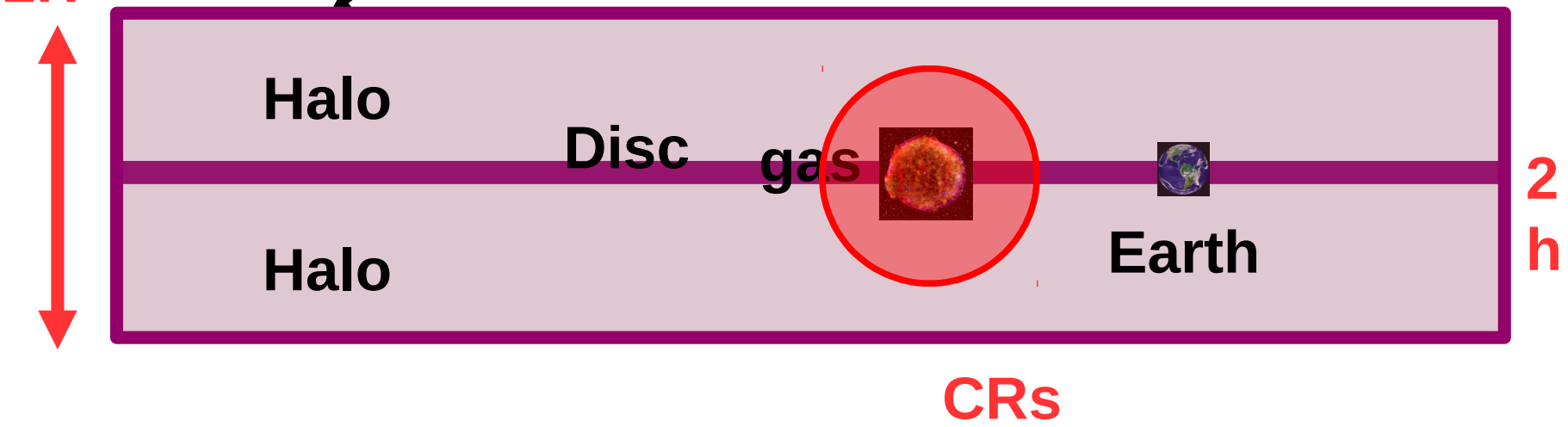

Grammage : $X = c\rho h H / D_z$ ~ several g/cm² at GeV

D ~ 10^{28} cm²/s at GeV **for H ~ several kpc**

~ GeV – TeV sky : Fermi

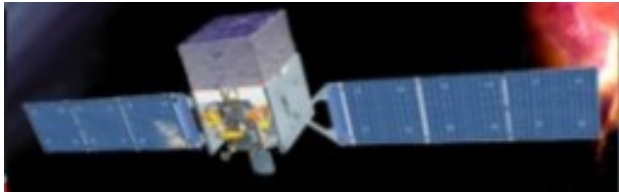

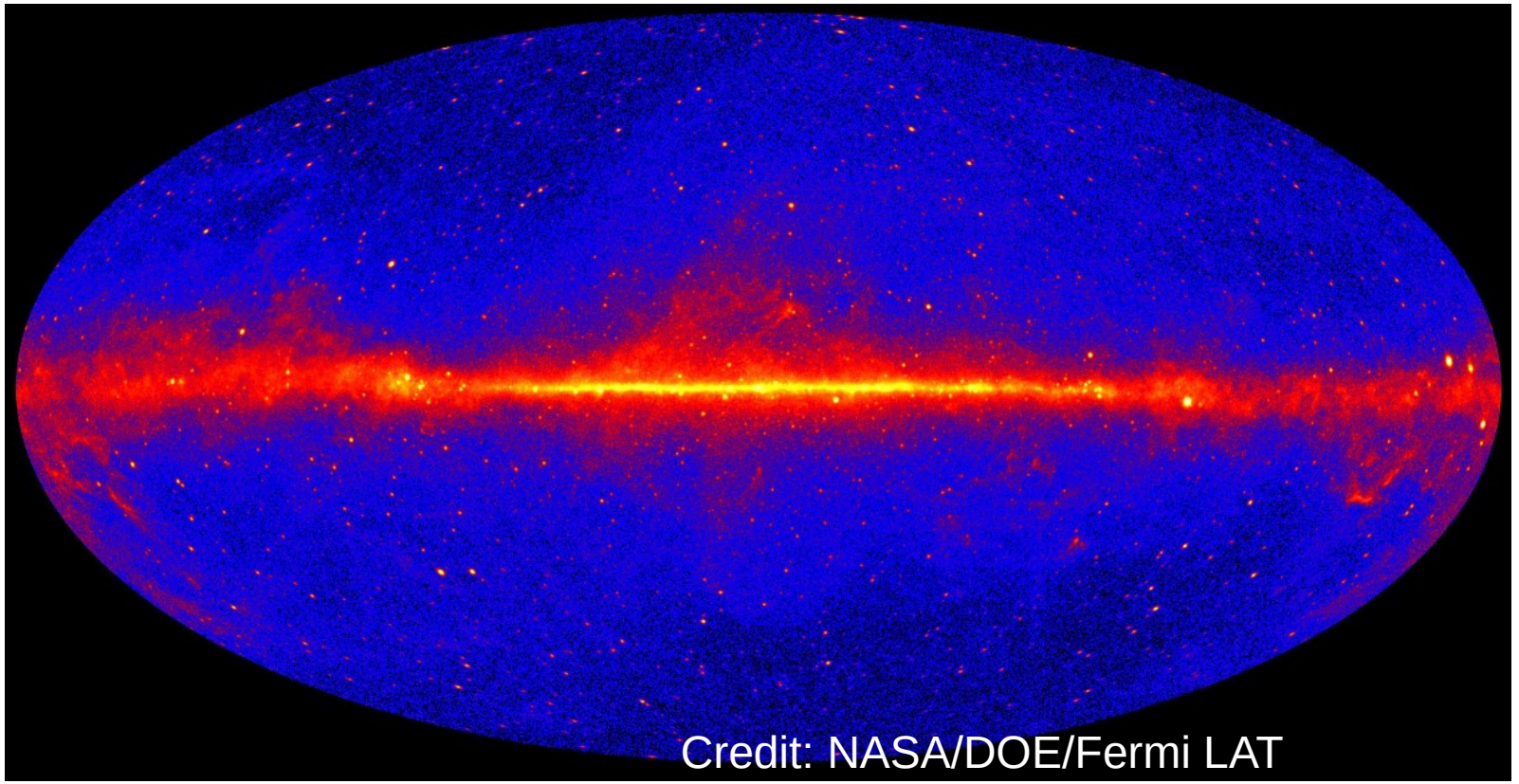

Diffuse emission: In agreement with SNR paradigm in terms of injected CR power.

PeV Gamma-Ray Astronomy: LHAASO

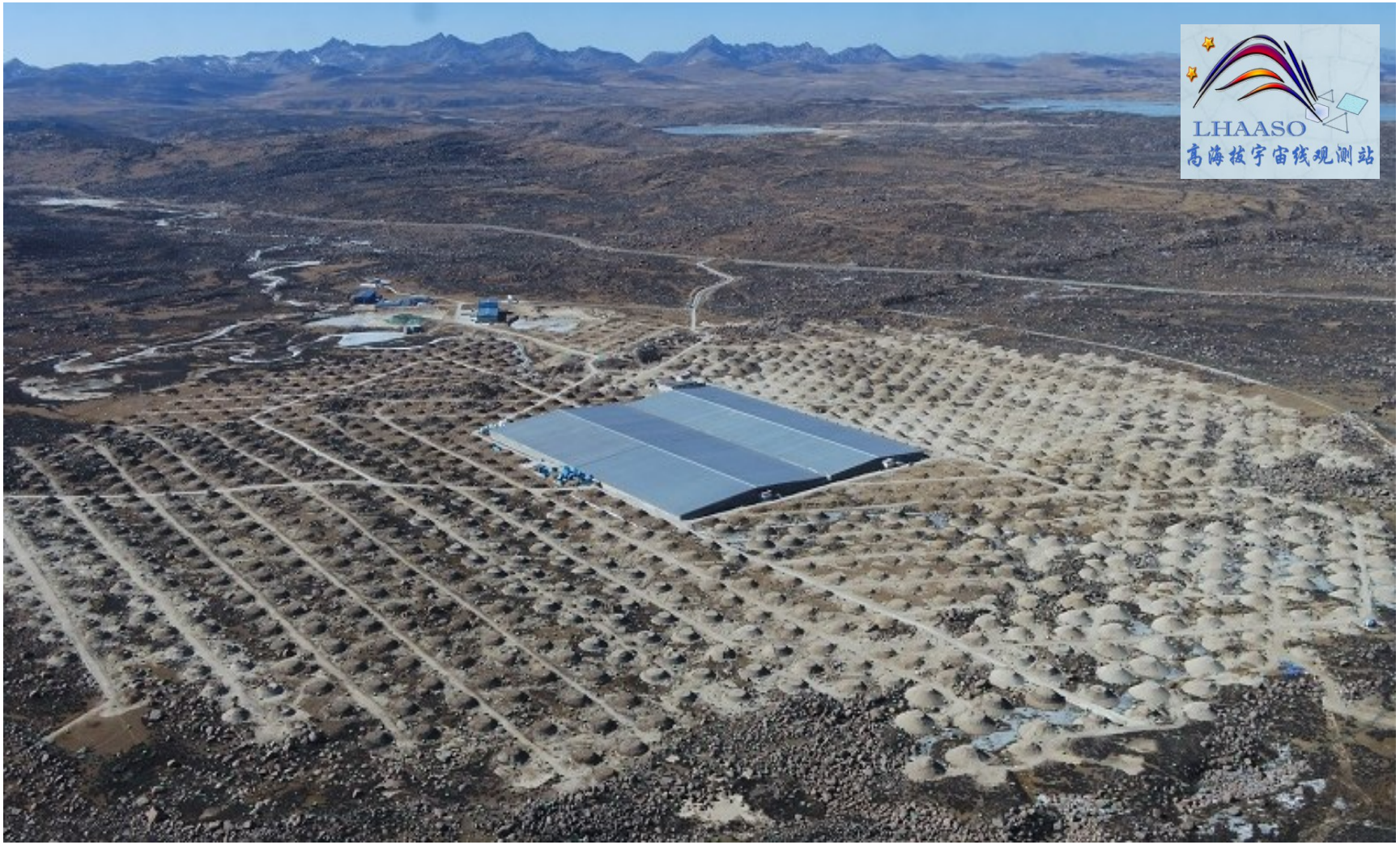

The sky at ~ 10 TeV – 1 PeV: Diffuse emission from LHAASO

LHAASO Collaboration, Phys. Rev. Lett. 131, 151001 (2023)

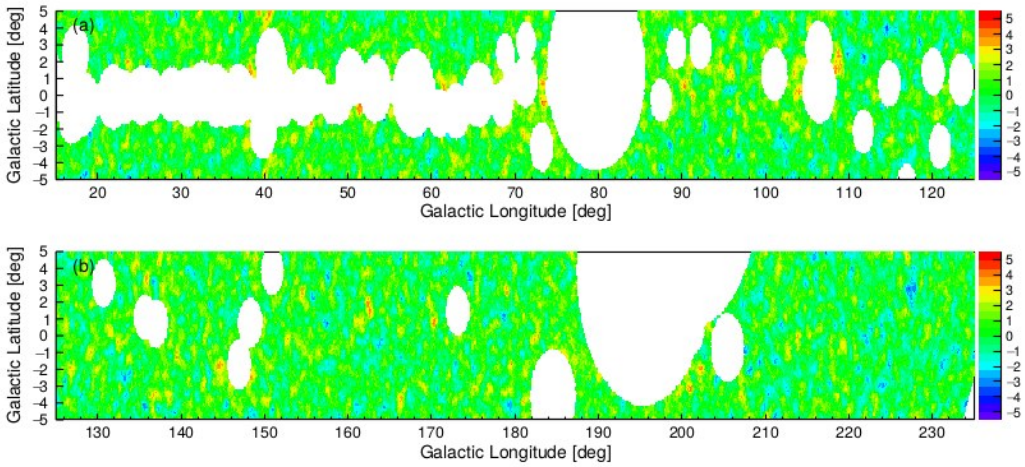

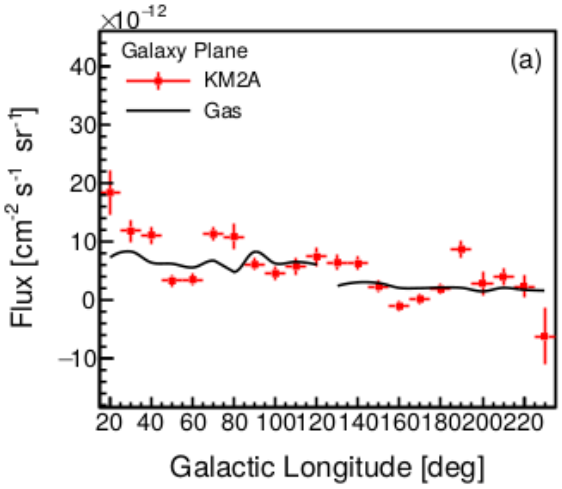

Emission in Galactic longitude does not follow target gas…

→ Leptonic origin?

→ Stochasticity of CR injection?

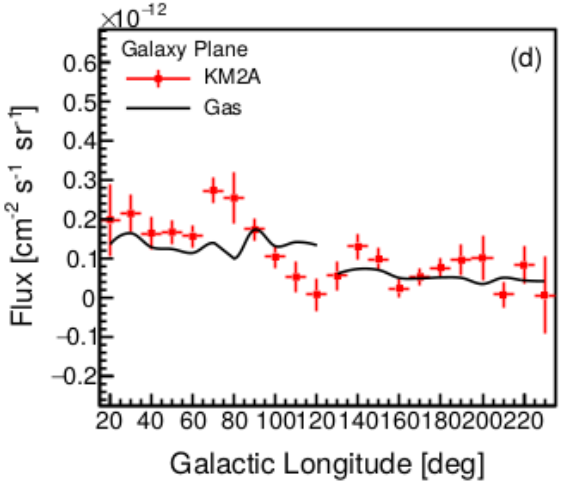

Sky at 25 TeV – 1 PeV with LHAASO

LHAASO Collaboration

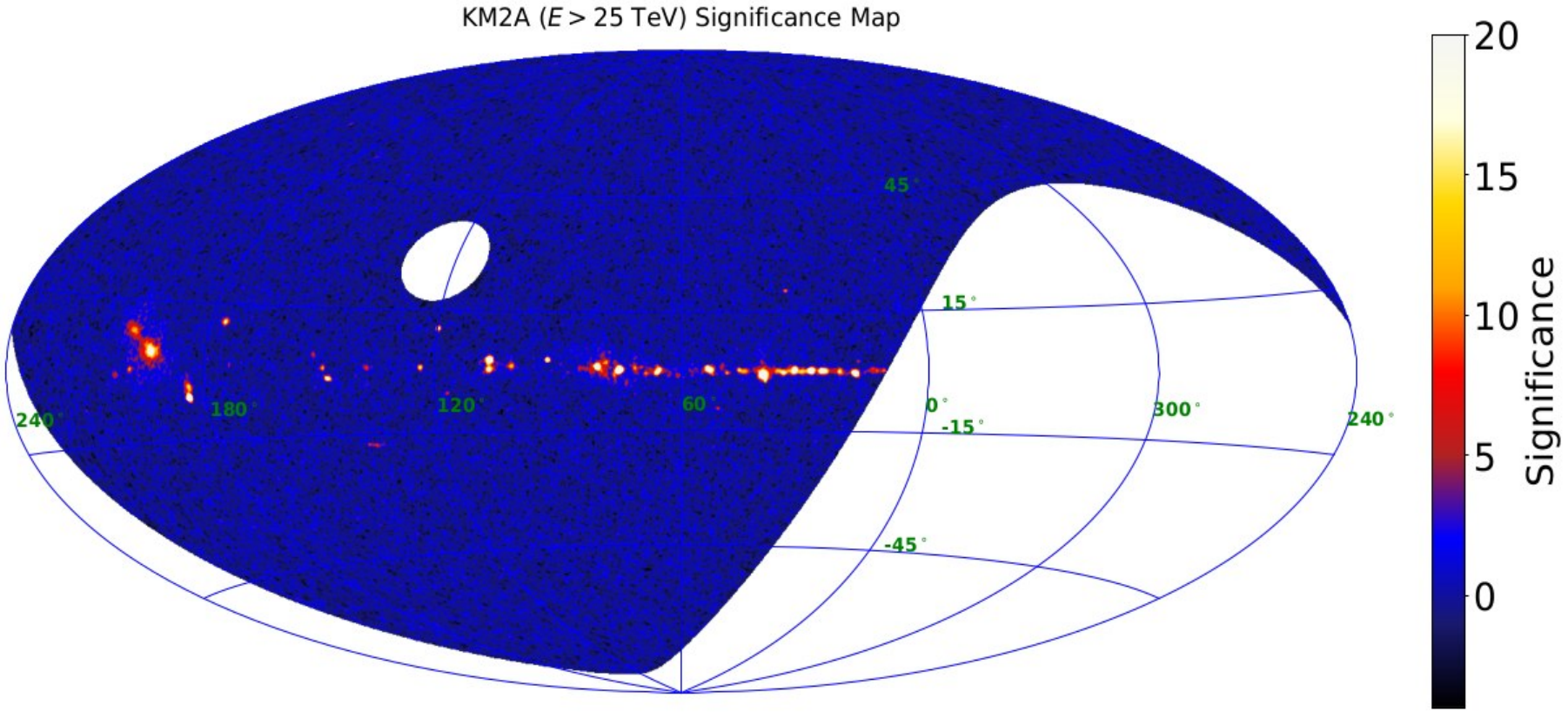

> Dozen of PeVatrons

~ 35 **PWNe & TeV Halos** (leptonic); ~ 7 **SNRs** (hadronic);
A **stellar cluster** (hadronic); 5 **Microquasars** (hadronic/leptonic?)

1 – TeV halos as a probe of CR propagation in the ISM

HAWC observ. of Geminga & Monogem

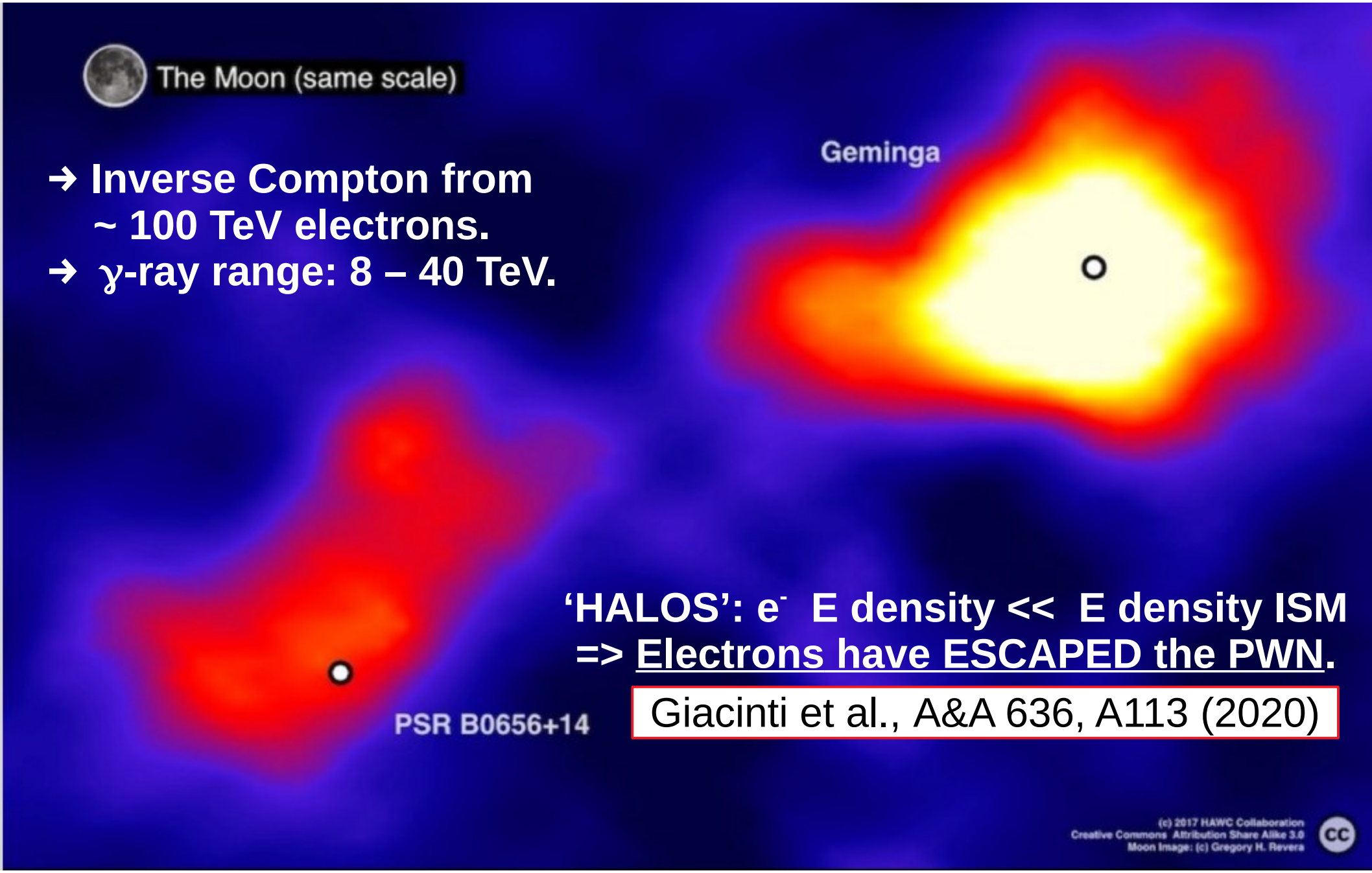

→ Inverse Compton from ~ 100 TeV electrons.

→ γ-ray range: 8 – 40 TeV.

'HALOS': e^- E density << E density ISM

=> Electrons have ESCAPED the PWN.

Giacinti et al., A&A 636, A113 (2020)

TeV Halos as probes of ISMF properties

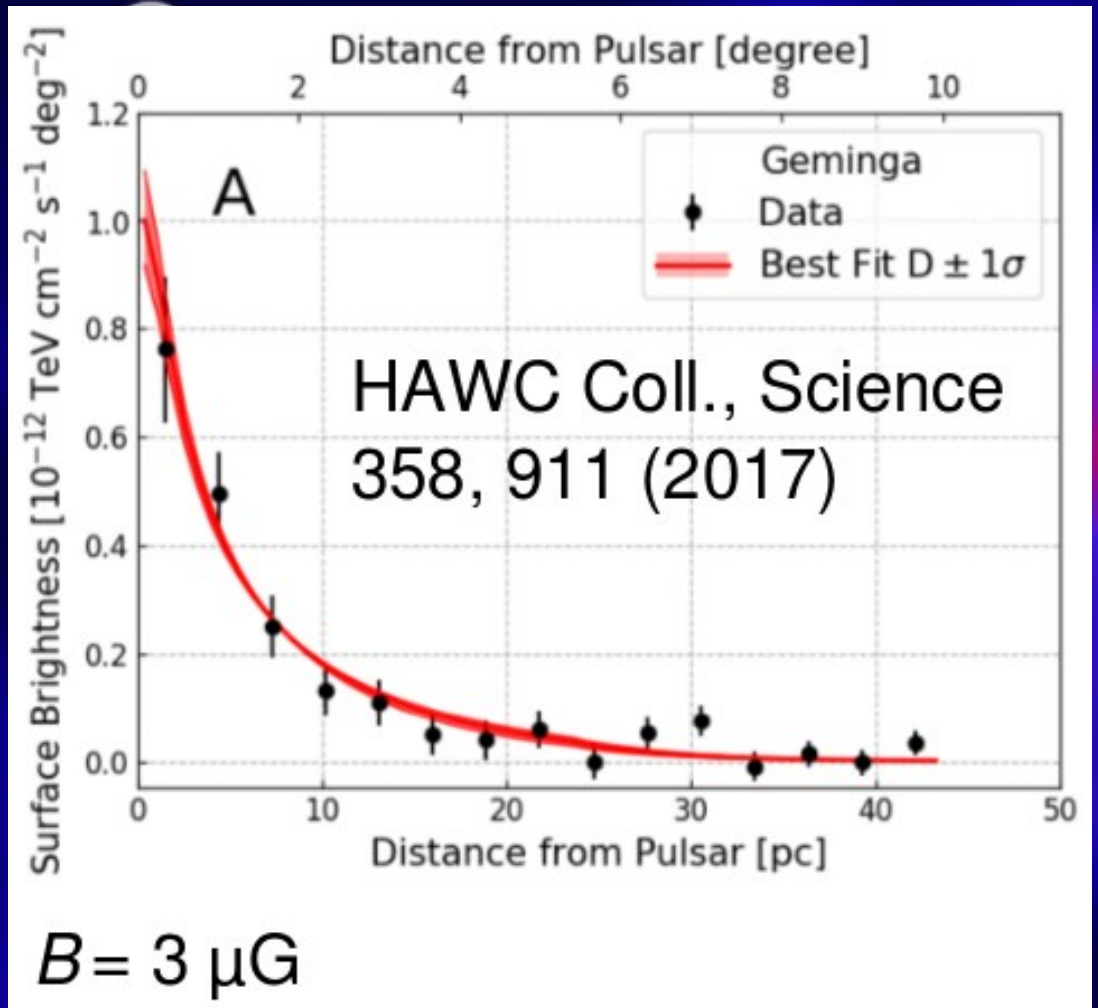

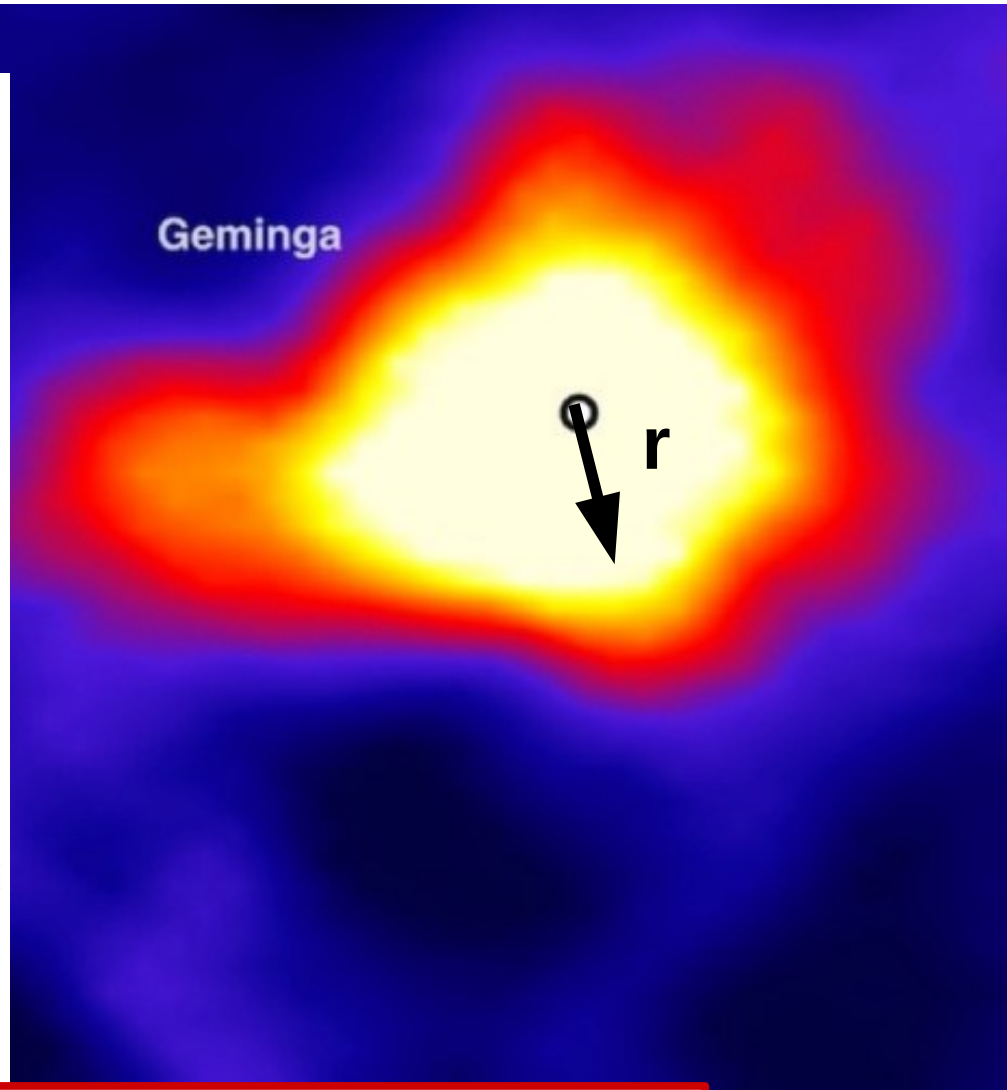

Best fit: **D(100 TeV) = 4.5 x 10^{27} cm^2/s**

2 orders of magnitude smaller than value from B/C ratio

PWNe & Potential TeV Halos in LHAASO Catalogue

Table 4. 1LHAASO sources associated pulsars

Source name	PSR name	Sep.(°)	d (kpc)	τ_c (kyr)	$\dot{E}$ (erg s^{-1})	P_c	Identified type in TeVCat
1LHAASO J0007+7303u	PSR J0007+7303	0.05	1.40	14	4.5e+35	7.3e-05	PWN
1LHAASO J0216+4237u	PSR J0218+4232	0.33	3.15	476000	2.4e+35	3.6e-03	
1LHAASO J0249+6022	PSR J0248+6021	0.16	2.00	62	2.1e+35	1.5e-03	
1LHAASO J0359+5406	PSR J0359+5414	0.15	-	75	1.3e+36	7.2e-04	
1LHAASO J0534+2200u	PSR J0534+2200	0.01	2.00	1	4.5e+38	3.2e-06	PWN
1LHAASO J0542+2311u	PSR J0543+2329	0.30	1.56	253	4.1e+34	8.3e-03	
1LHAASO J0622+3754	PSR J0622+3749	0.09	-	208	2.7e+34	2.5e-04	PWN/TeV Halo
1LHAASO J0631+1040	PSR J0631+1037	0.11	2.10	44	1.7e+35	3.5e-04	PWN
1LHAASO J0634+1741u	PSR J0633+1746	0.12	0.19	342	3.3e+34	1.3e-03	PWN/TeV Halo
1LHAASO J0635+0619	PSR J0633+0632	0.39	1.35	59	1.2e+35	9.4e-03	
1LHAASO J1740+0948u	PSR J1740+1000	0.21	1.23	114	2.3e+35	1.4e-03	
1LHAASO J1809-1918u	PSR J1809-1917	0.05	3.27	51	1.8e+36	6.2e-04	
1LHAASO J1813-1245	PSR J1813-1245	0.01	2.63	43	6.2e+36	6.3e-06	
1LHAASO J1825-1256u	PSR J1826-1256	0.09	1.55	14	3.6e+36	1.6e-03	
1LHAASO J1825-1337u	PSR J1826-1334	0.11	3.61	21	2.8e+36	2.8e-03	PWN/TeV Halo
1LHAASO J1837-0654u	PSR J1838-0655	0.12	6.60	23	5.6e+36	2.2e-03	PWN
1LHAASO J1839-0548u	PSR J1838-0537	0.20	-	5	6.0e+36	6.1e-03	
1LHAASO J1848-0001u	PSR J1849-0001	0.06	-	43	9.8e+36	1.2e-04	PWN
1LHAASO J1857+0245	PSR J1856+0245	0.16	6.32	21	4.6e+36	3.1e-03	PWN
1LHAASO J1906+0712	PSR J1906+0722	0.19	-	49	1.0e+36	5.9e-03	
1LHAASO J1908+0615u	PSR J1907+0602	0.23	2.37	20	2.8e+36	6.8e-03	
1LHAASO J1912+1014u	PSR J1913+1011	0.13	4.61	169	2.9e+36	1.5e-03	
1LHAASO J1914+1150u	PSR J1915+1150	0.09	14.01	116	5.4e+35	1.8e-03	
1LHAASO J1928+1746u	PSR J1928+1746	0.04	4.34	83	1.6e+36	1.6e-04	
1LHAASO J1929+1846u	PSR J1930+1852	0.29	7.00	3	1.2e+37	2.6e-03	PWN
1LHAASO J1954+2836u	PSR J1954+2836	0.01	1.96	69	1.1e+36	1.6e-05	PWN
1LHAASO J1954+3253	PSR J1952+3252	0.33	3.00	107	3.7e+36	6.7e-03	
1LHAASO J1959+2846u	PSR J1958+2845	0.10	1.95	22	3.4e+35	2.8e-03	PWN
1LHAASO J2005+3415	PSR J2004+3429	0.25	10.78	18	5.8e+35	9.9e-03	
1LHAASO J2005+3050	PSR J2006+3102	0.20	6.04	104	2.2e+35	9.2e-03	
1LHAASO J2020+3649u	PSR J2021+3651	0.05	1.80	17	3.4e+36	1.5e-04	PWN
1LHAASO J2028+3352	PSR J2028+3332	0.36	-	576	3.5e+34	8.0e-03	
1LHAASO J2031+4127u	PSR J2032+4127	0.08	1.33	201	1.5e+35	1.0e-03	PWN
1LHAASO J2228+6100u	PSR J2229+6114	0.27	3.00	10	2.2e+37	2.2e-03	PWN
1LHAASO J2238+5900	PSR J2238+5903	0.07	2.83	27	8.9e+35	3.0e-04	

LHAASO Collaboration, ApJS 271, 25 (2024)

Evolutionary stages of a PWN :

Giacinti, Mitchell, Lopez-Coto, Joshi, Parsons & Hinton,
A&A 636, A113 (2020), arXiv:1907.12121:

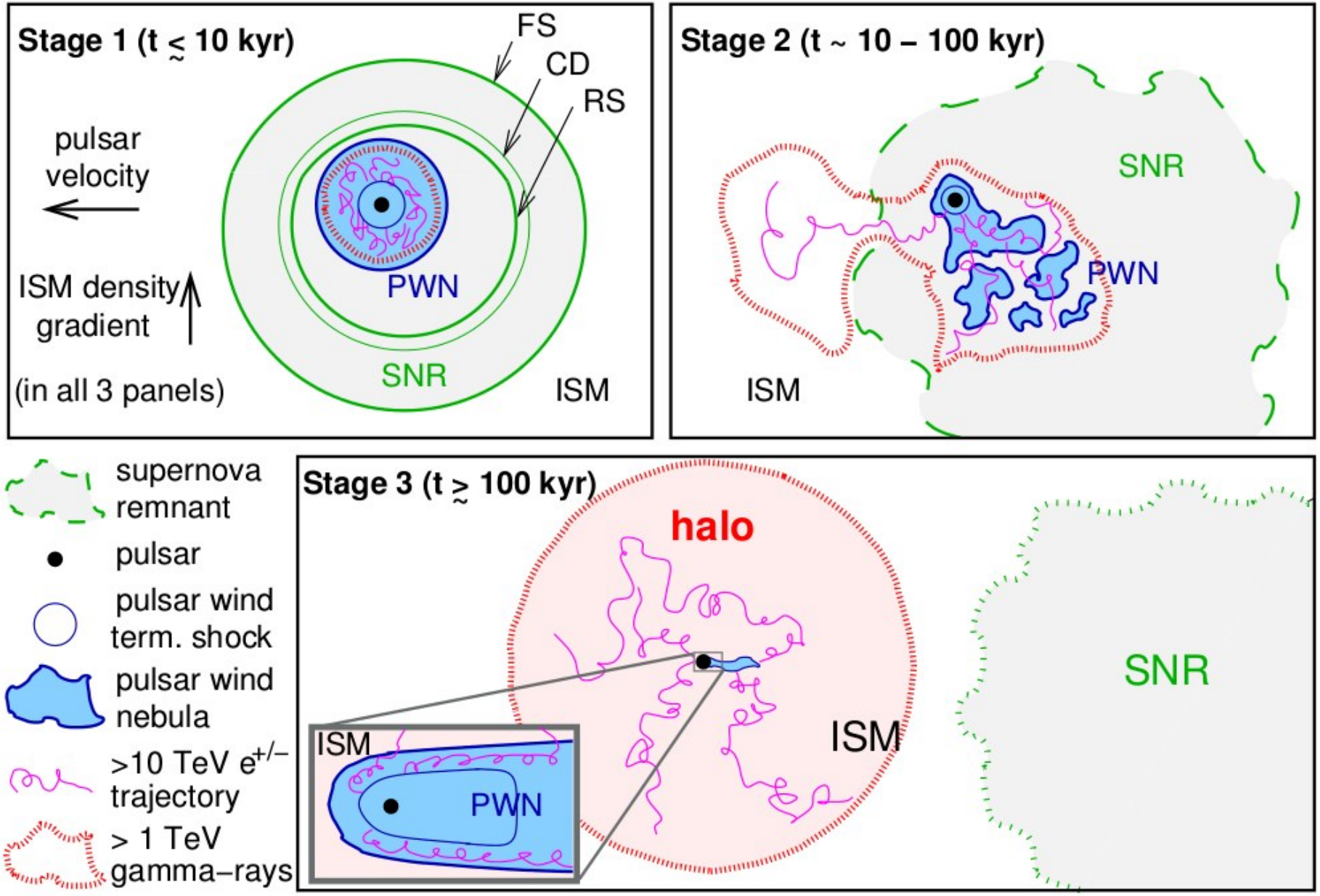

Predicted γ-ray surface brightness

Kolmogorov, B_{rms}=3 μG, **L_c = 5 pc** :

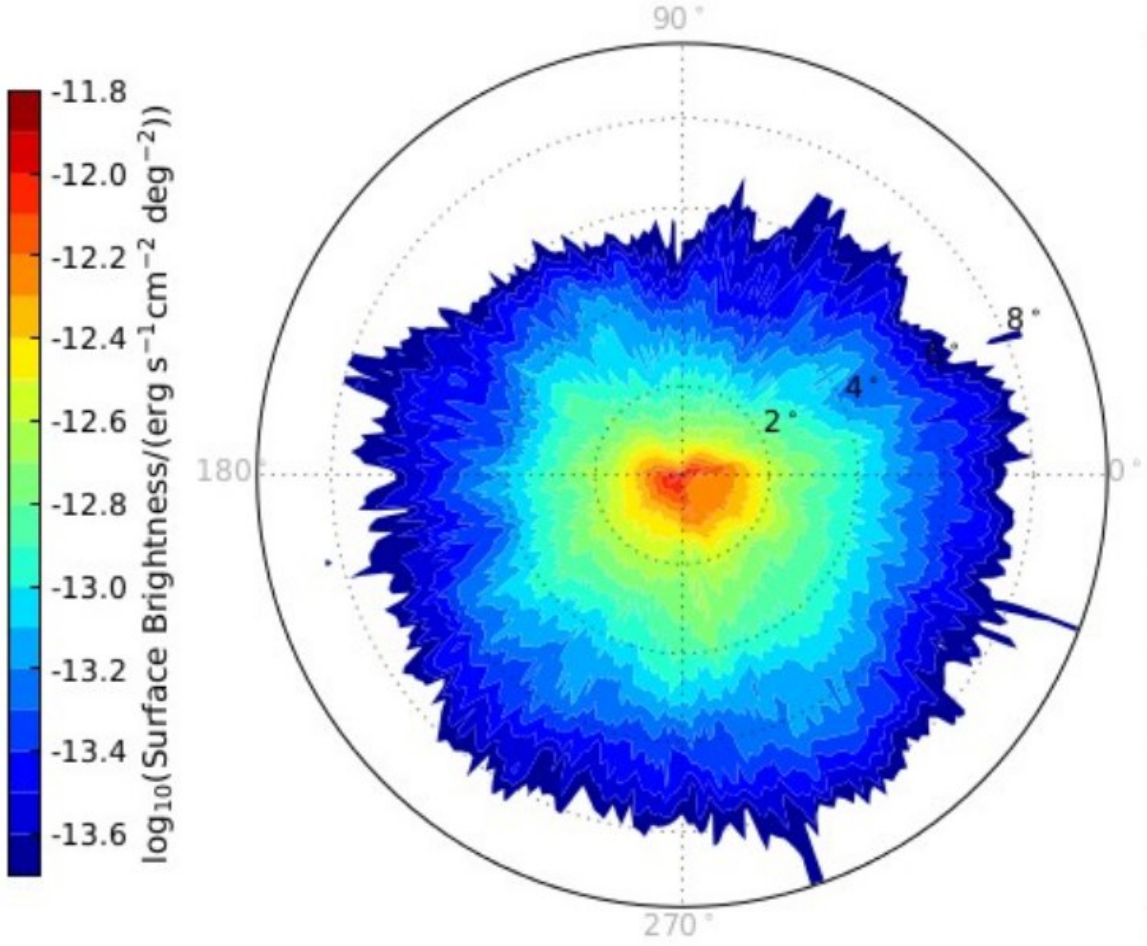

OK

Lopez-Coto & Giacinti, MNRAS 479, 4526 (2018) [arXiv:1712.04373]

Predicted γ-ray surface brightness

Kolmogorov, B_{rms}=3 μG, **L_c = 40 pc** :

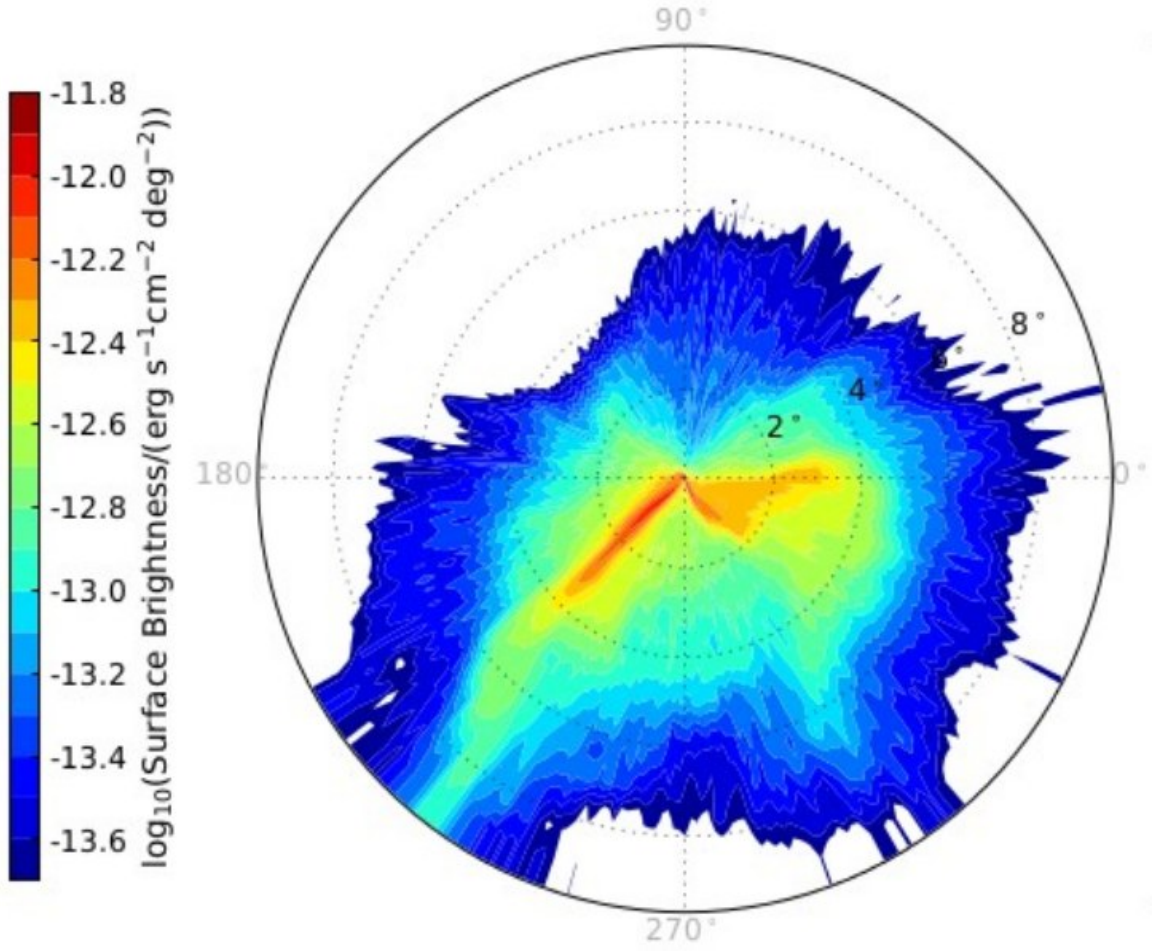

INCOMPATIBLE WITH HAWC MEASUREMENTS

Large coherence lengths (> 10 pc) ruled out (Too asymmetric)

Best fit to HAWC measurements (χ^2/ndf<1)

→ Kolmogorov / Kraichnan, B = 3 μG, L_c = 1 pc

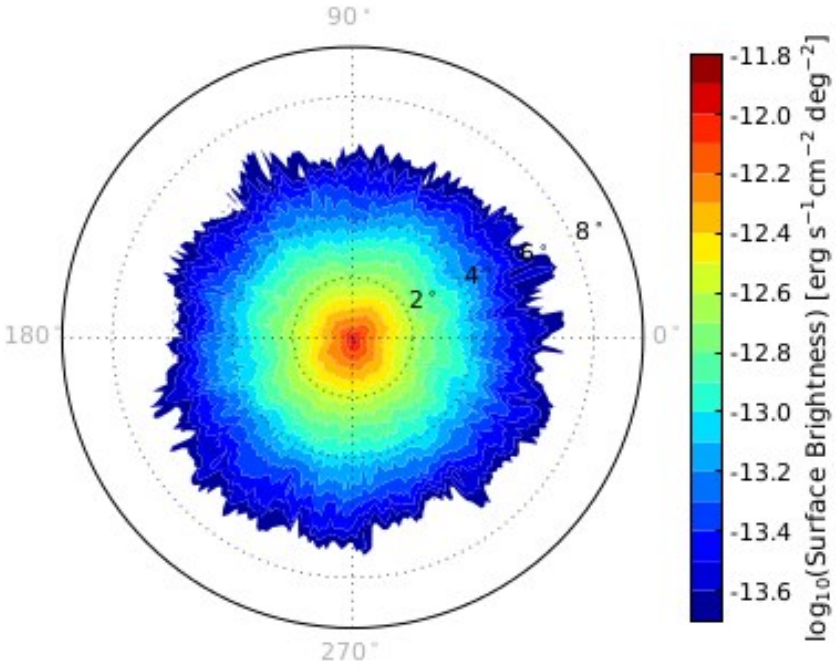

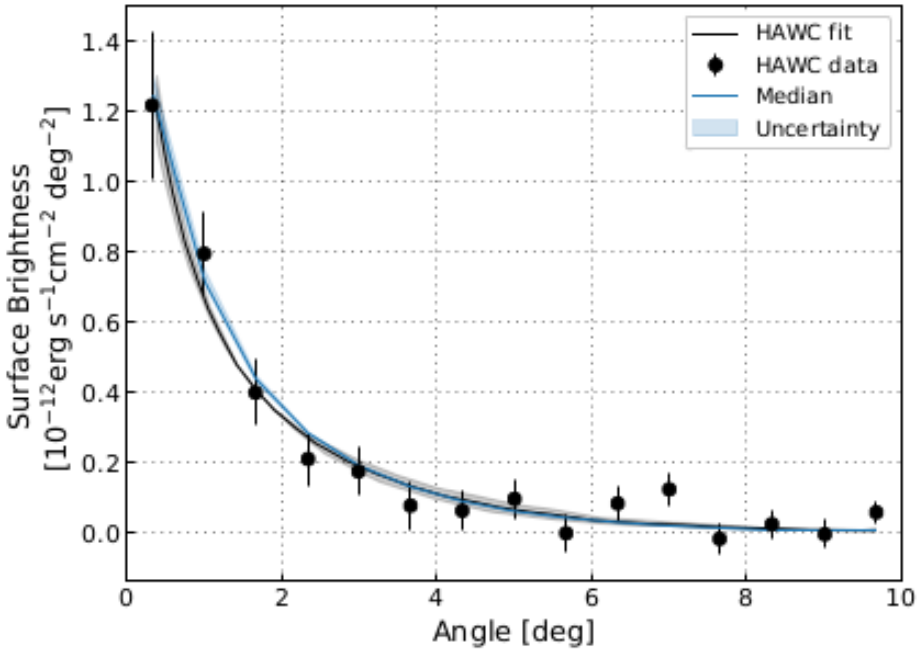

Lopez-Coto & Giacinti, MNRAS 479, 4526 (2018) [arXiv:1712.04373]

Li, Giacinti & Lopez-Coto, To be submitted (2025)

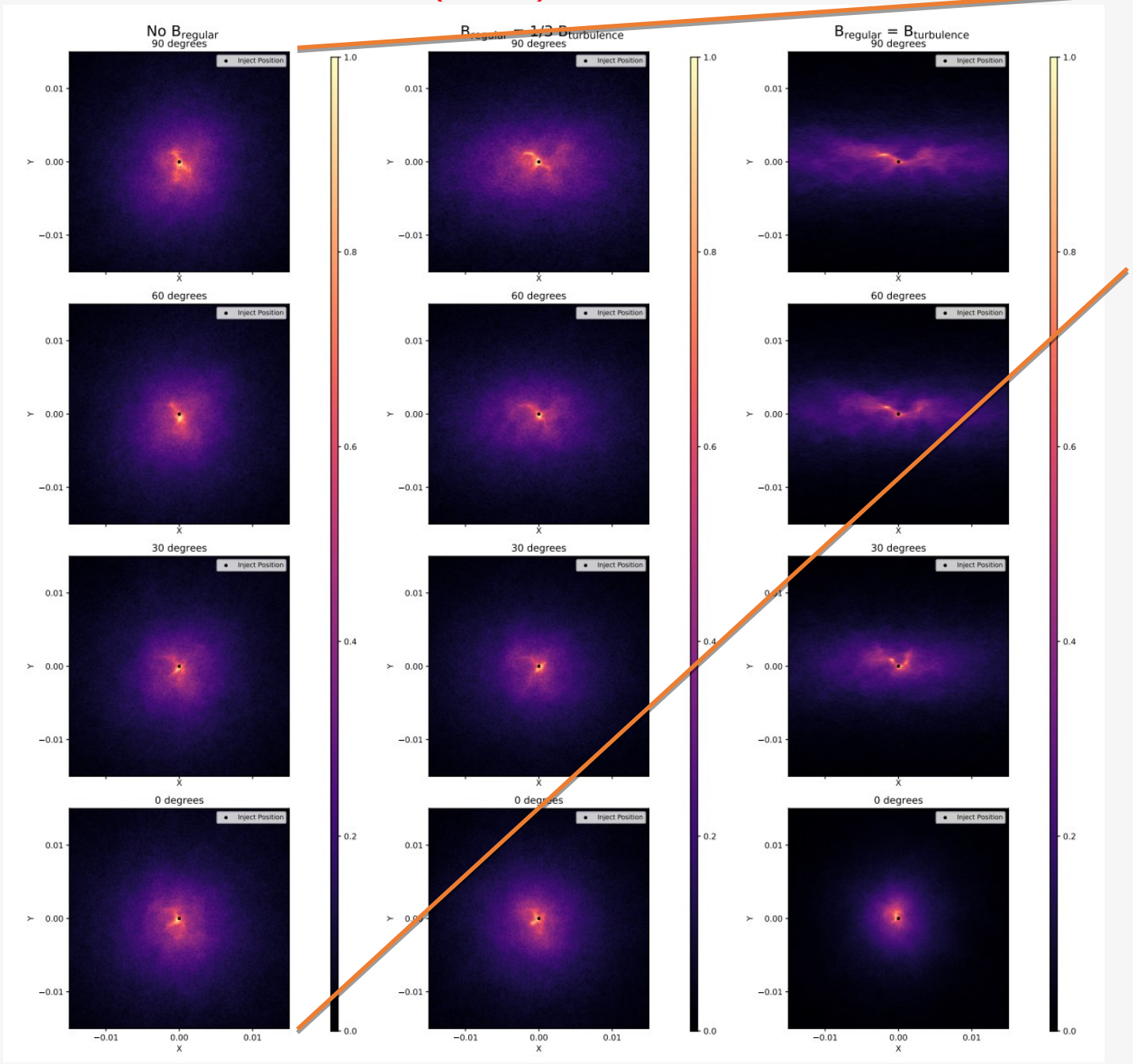

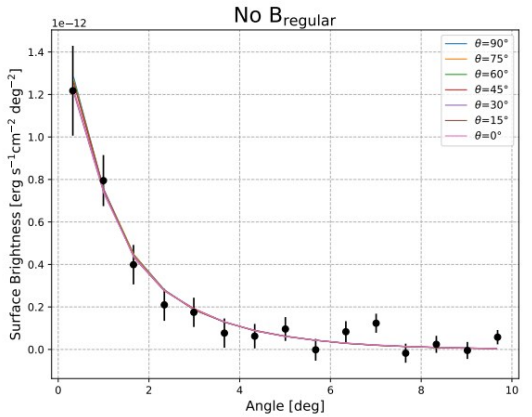

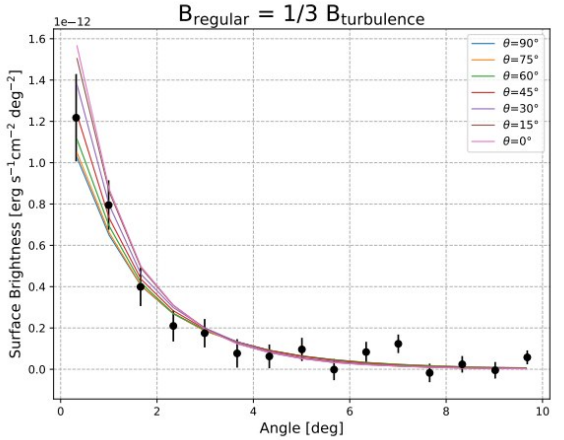

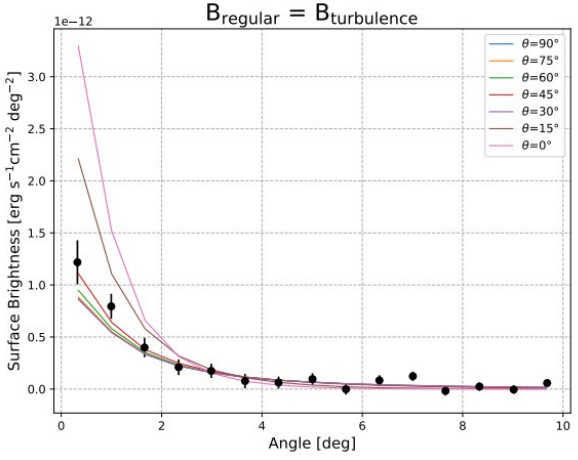

Best fits around
L_c=1-5 pc,
B_{rms}=3-4 μG

Kolmogorov,
L_c=1 pc,
B_{rms}=3 μG

Asymmetry results ($B_{regular} = 0$):

Li, Giacinti & Lopez-Coto, To be submitted (2025)

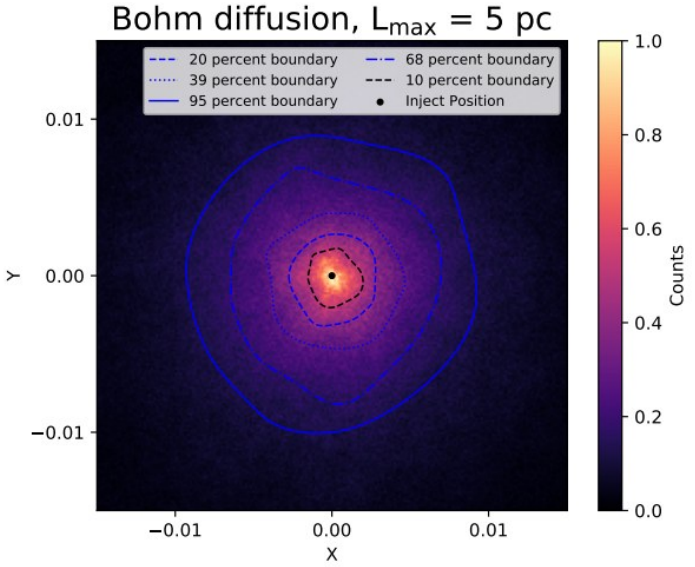

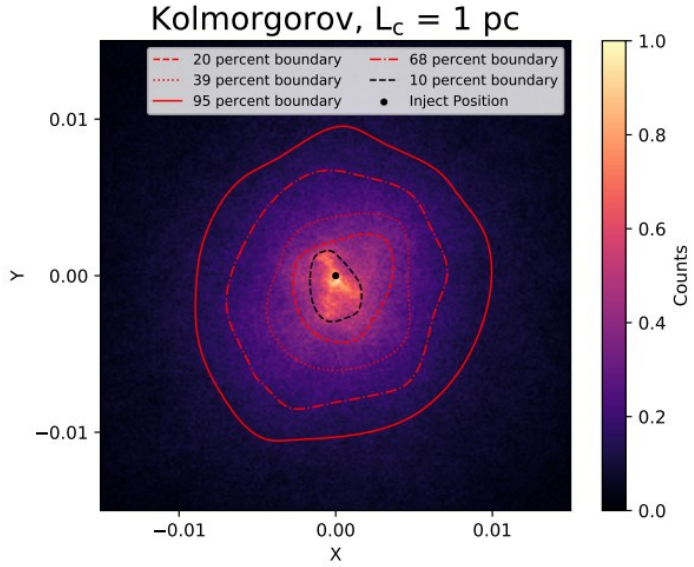

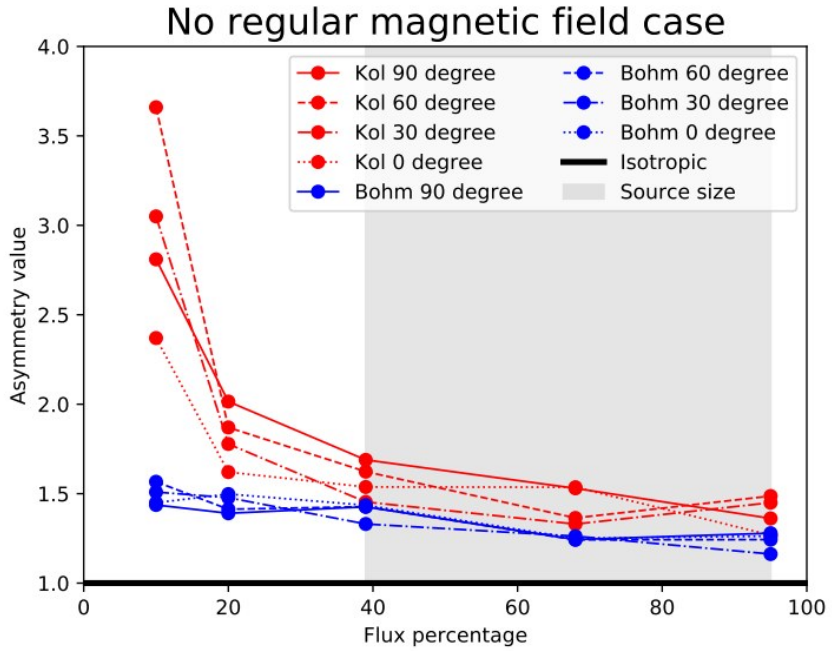

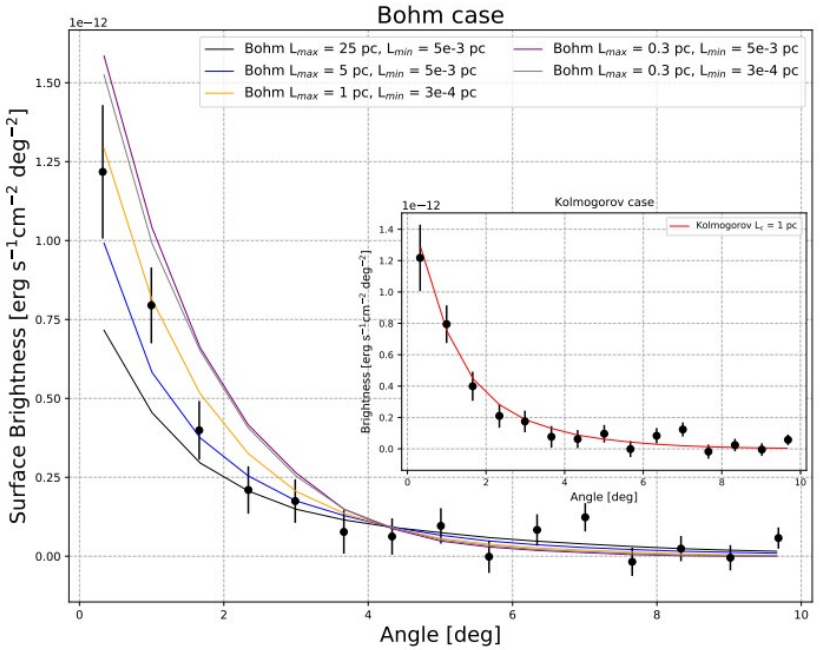

Or could the local L_c be >> 10 pc ?

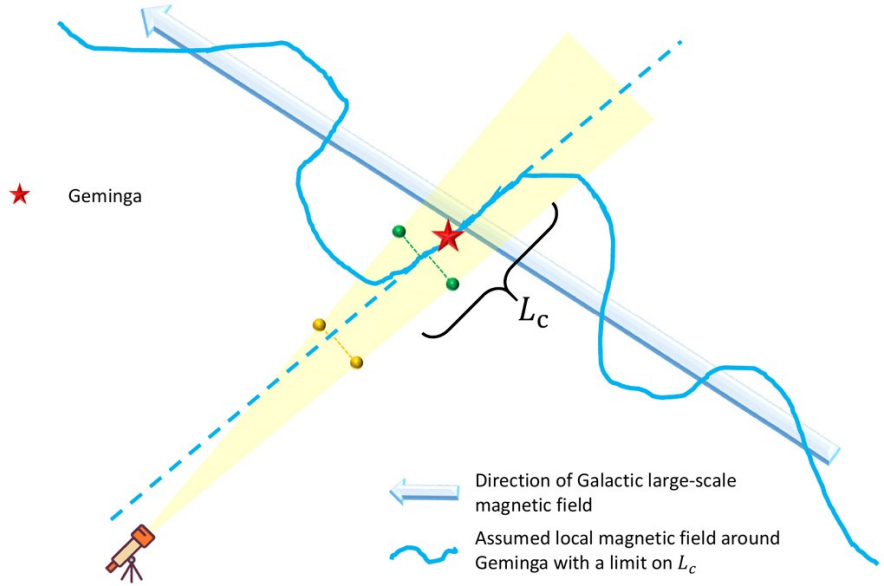

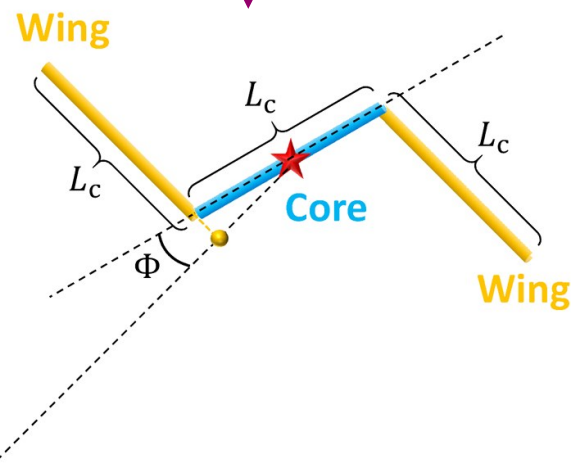

Fang et al., PRD (2023)

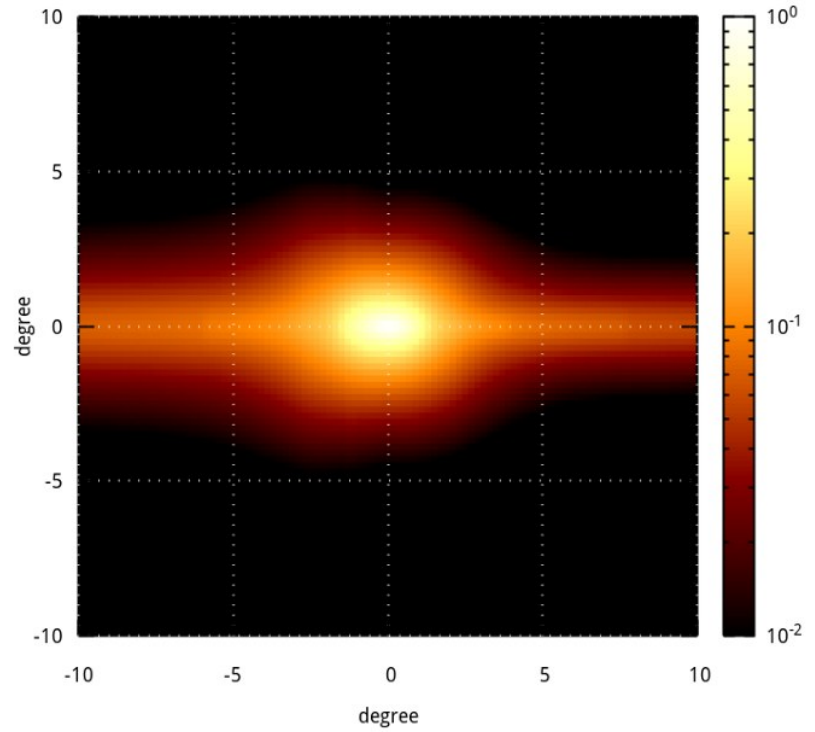

Large coherence lengths:

Li, Giacinti & Lopez-Coto, To be submitted (2025)

L c = 100 pc and B rms = 3 μG

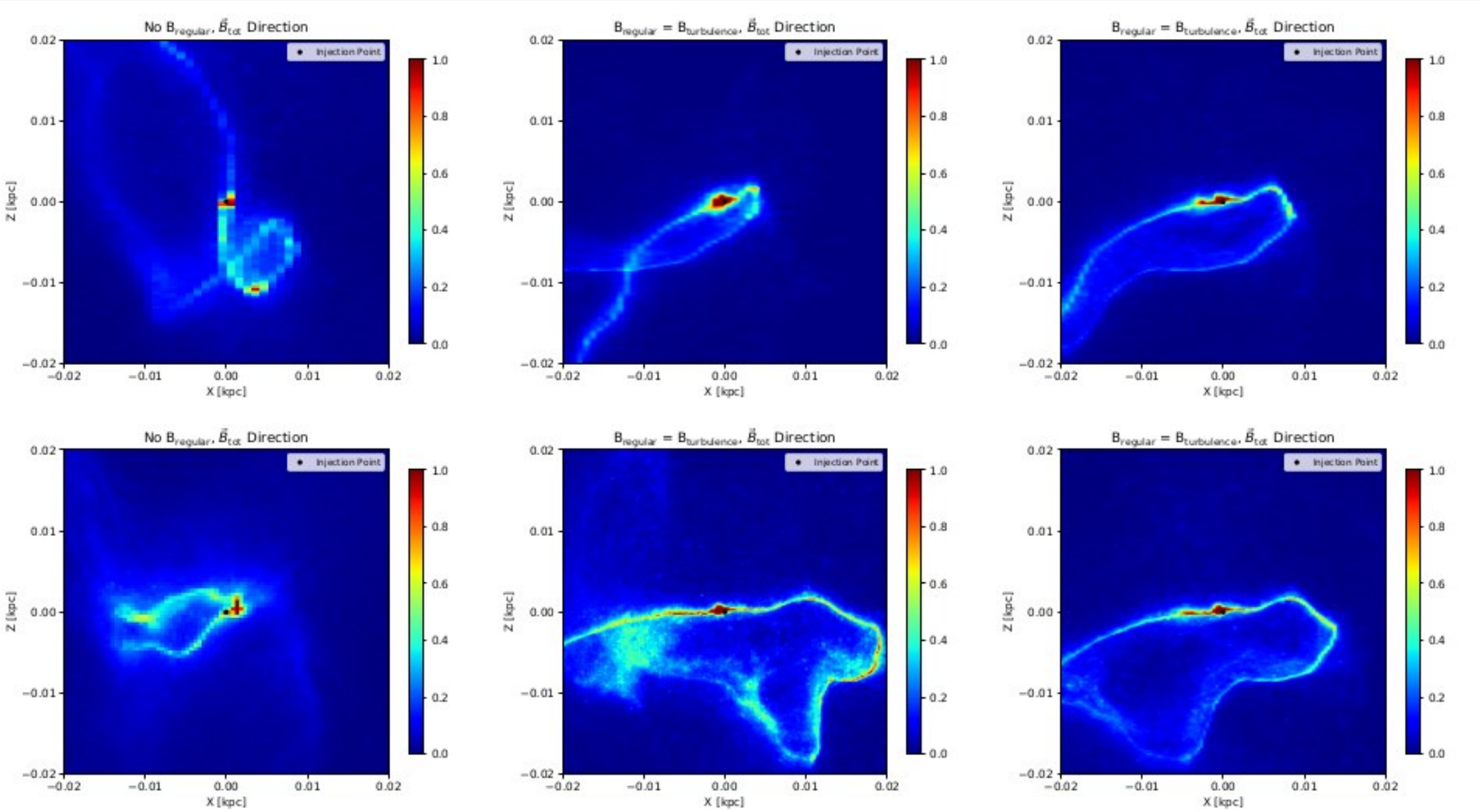

Appearance of “mirage” sources:

They may appear around astrophysical sources.

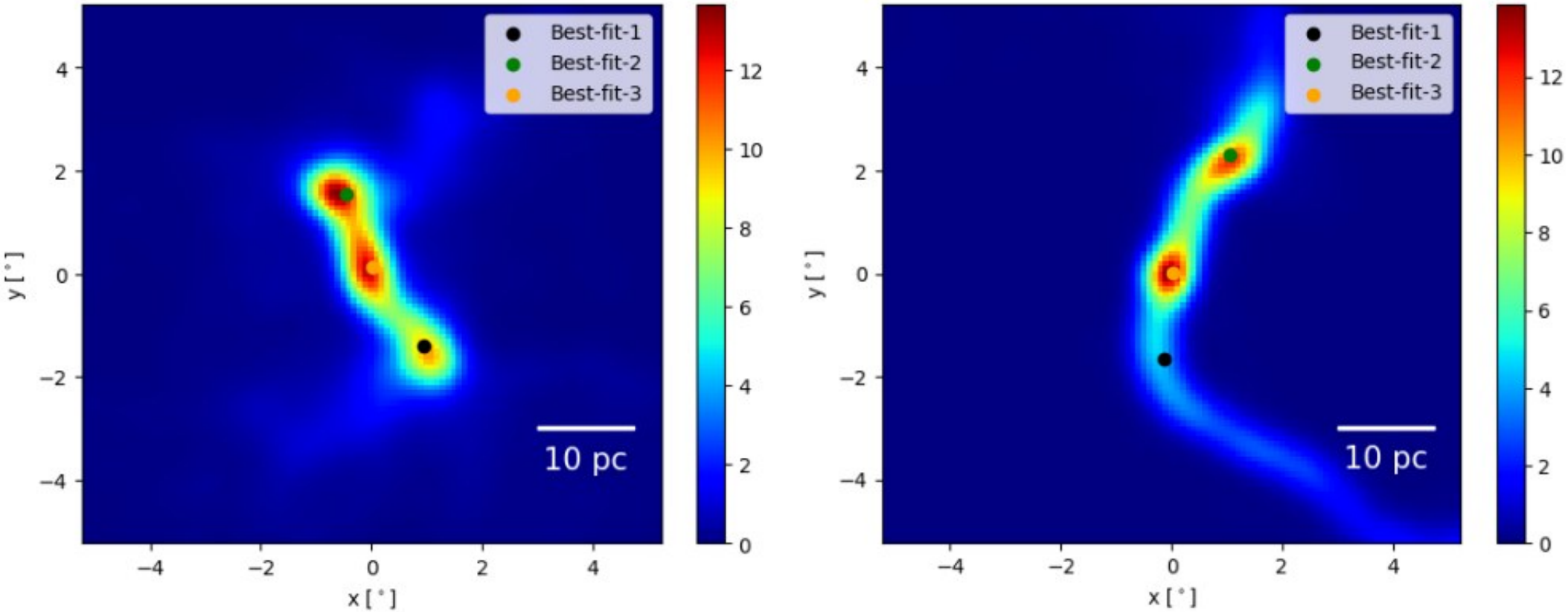

L_c = 40pc ; B_{turb} = 3 μG ; B_{reg} = 0 μG; Kolmogorov turbulence ; (8192 particles)

Bao, Giacinti, Liu, Zhang & Chen, Phys. Rev. Lett. (2025)
Bao, Liu, Giacinti, Zhang & Chen, Phys. Rev. D (2025)

Could explain LHAASO observations

LHAASO Collaboration, ApJS 271, 25 (2024)

Many **extended sources** w/ **irregular shapes:**

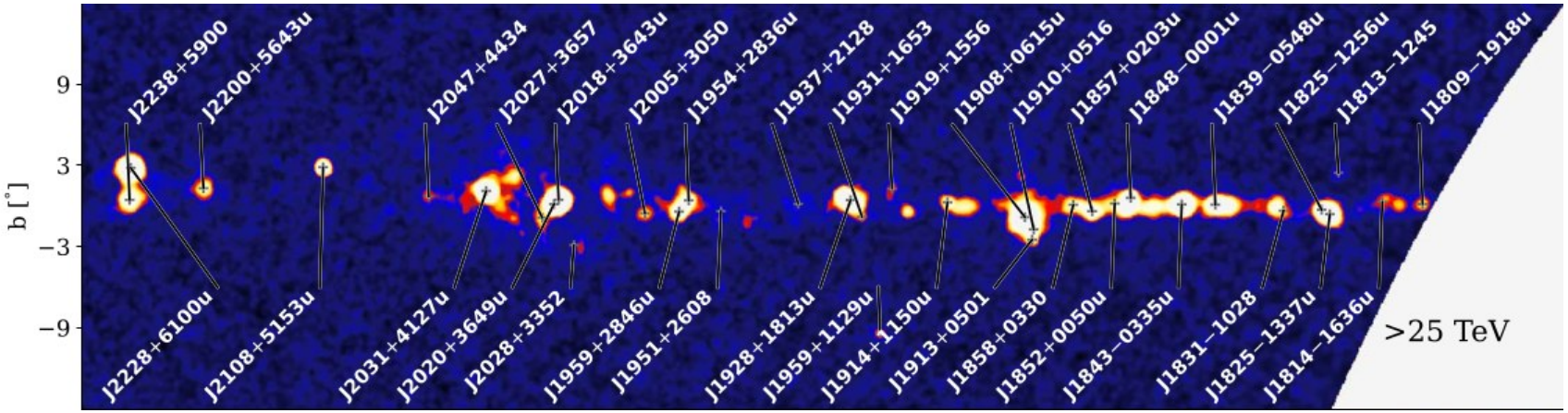

Large offsets between sources and center

Table 4. 1LHAASO sources associated pulsars

Source name	PSR name	Sep.(°)	d (kpc)	τ_c (kyr)	$\dot{E}$ (erg s^{-1})	P_c	Identified type in TeVCat
1LHAASO J0007+7303u	PSR J0007+7303	0.05	1.40	14	4.5e+35	7.3e-05	PWN
1LHAASO J0216+4237u	PSR J0218+4232	0.33	3.15	476000	2.4e+35	3.6e-03	
1LHAASO J0249+6022	PSR J0248+6021	0.16	2.00	62	2.1e+35	1.5e-03	
1LHAASO J0359+5406	PSR J0359+5414	0.15	-	75	1.3e+36	7.2e-04	
1LHAASO J0534+2200u	PSR J0534+2200	0.01	2.00	1	4.5e+38	3.2e-06	PWN
1LHAASO J0542+2311u	PSR J0543+2329	0.30	1.56	253	4.1e+34	8.3e-03	
1LHAASO J0622+3754	PSR J0622+3749	0.09	-	208	2.7e+34	2.5e-04	PWN/TeV Halo
1LHAASO J0631+1040	PSR J0631+1037	0.11	2.10	44	1.7e+35	3.5e-04	PWN
1LHAASO J0634+1741u	PSR J0633+1746	0.12	0.19	342	3.3e+34	1.3e-03	PWN/TeV Halo
1LHAASO J0635+0619	PSR J0633+0632	0.39	1.35	59	1.2e+35	9.4e-03	
1LHAASO J1740+0948u	PSR J1740+1000	0.21	1.23	114	2.3e+35	1.4e-03	

LHAASO's peanut-shaped source

LHAASO Coll., arXiv:2510.06786

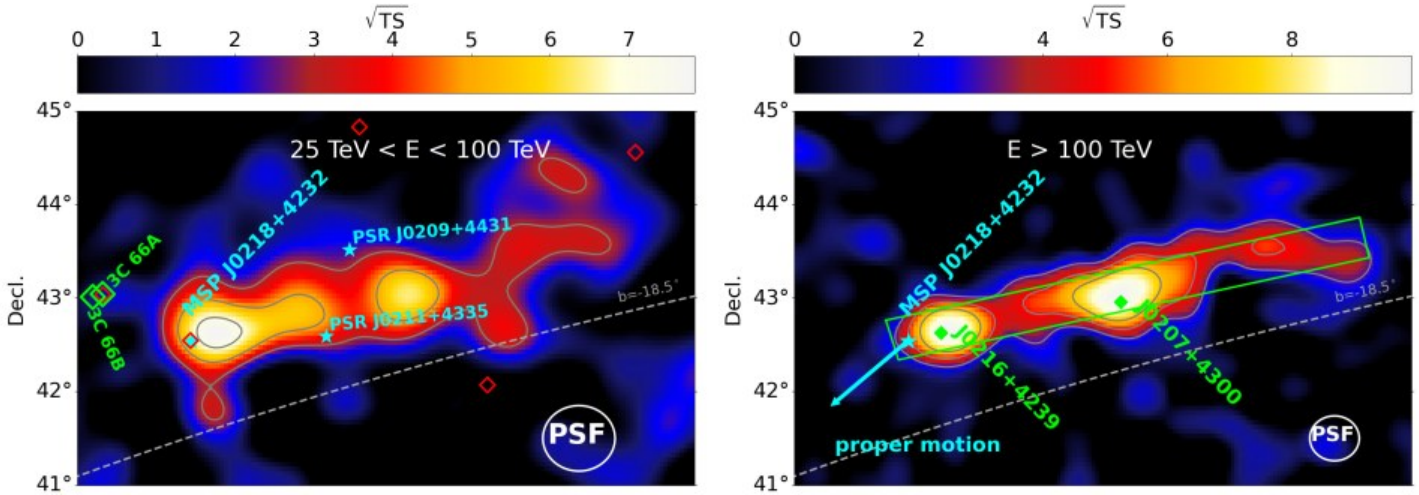

GG et al., In prep (2026)

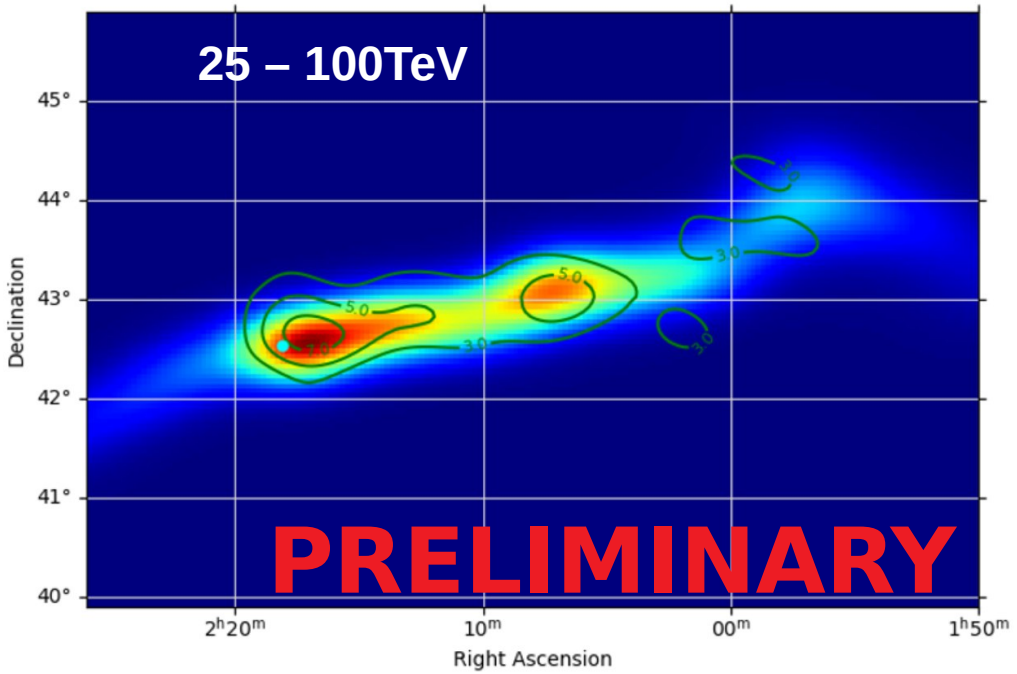

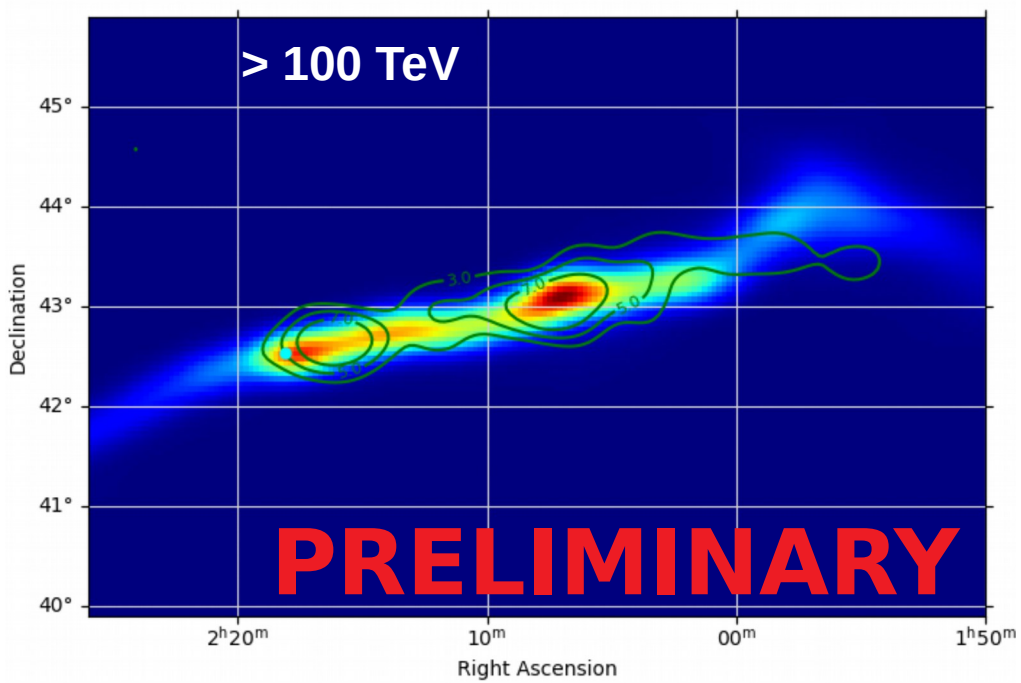

2 – Diffuse VHE γ-ray emission:

Impact of unresolved sources (PWNe)

Kaci, Giacinti, Semikoz, ApJ Lett. 975, L6 (2024)

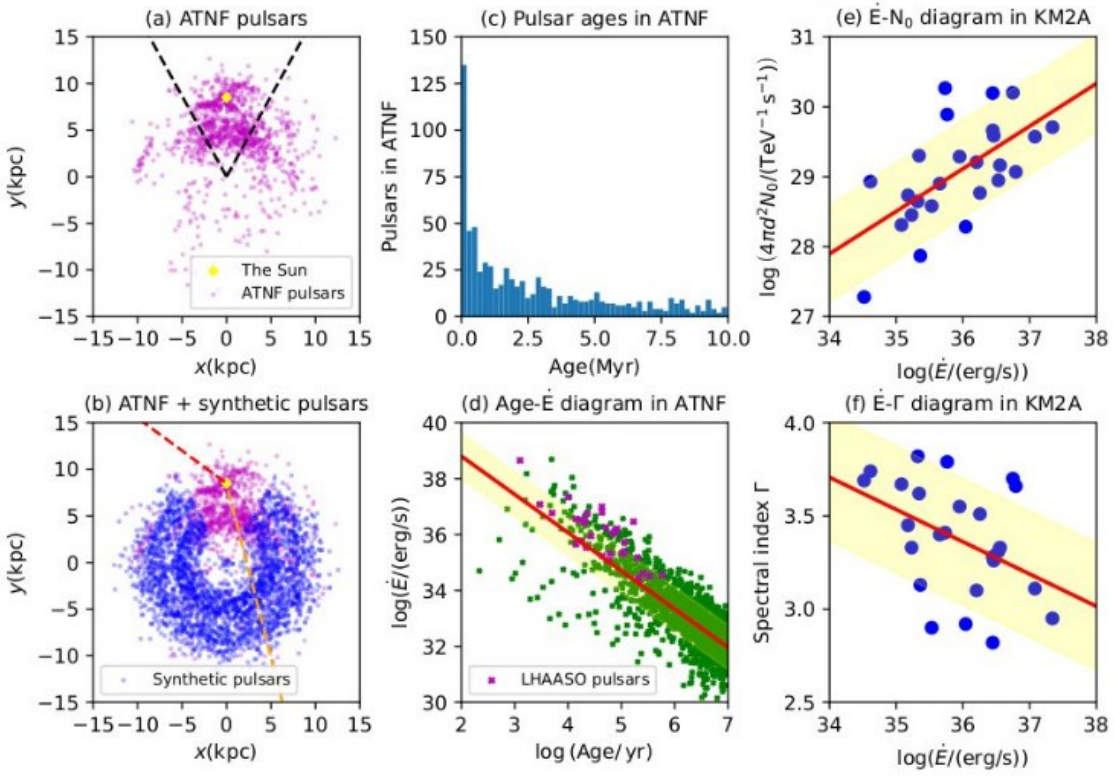

- Use ATNF catalog and complete it.
- Generate a VHE gamma-ray emission similar to that measured by KM2A for each source.
- Constrain the gamma-ray emission to be below KM2A sensitivity.
- Use the same masks as LHAASO.
- Compare the contribution of unresolved sources to the total flux measured by KM2A.

Upper Limits unresolved PWNe/halos

Kaci, Giacinti, Semikoz,
ApJ Lett. 975, L6 (2024)

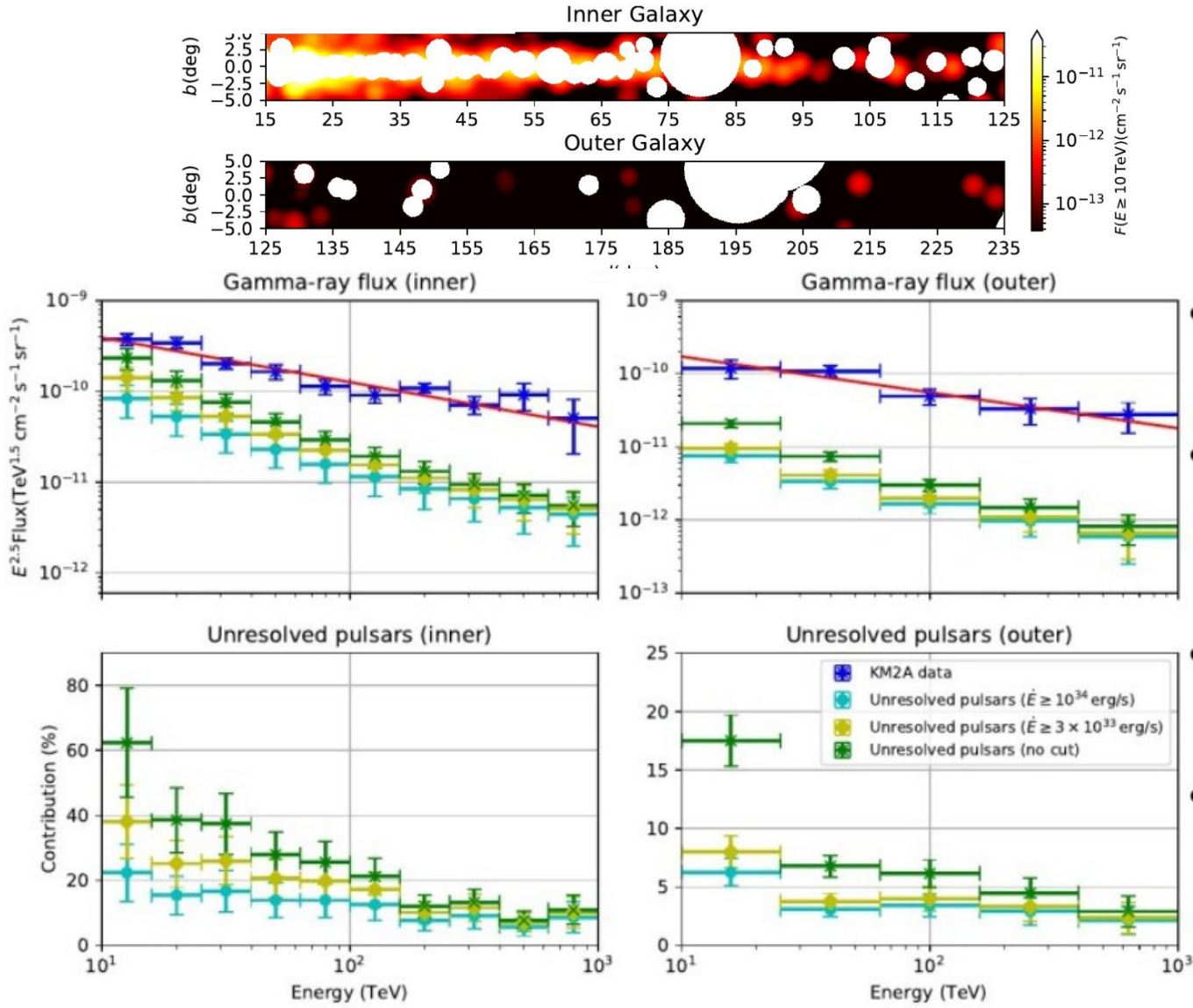

Upper Limits unresolved PWNe/halos

Kaci, Giacinti, Semikoz, Submitted (2026)

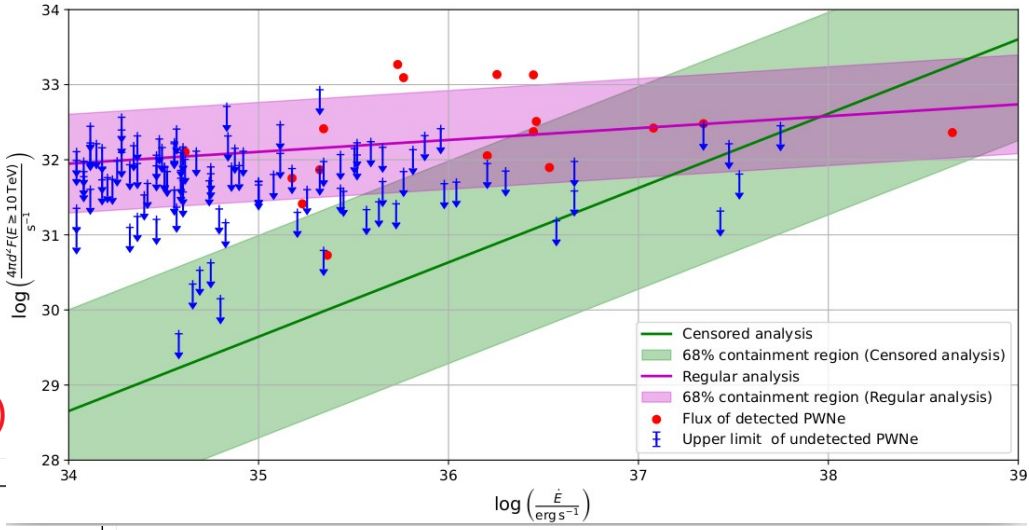

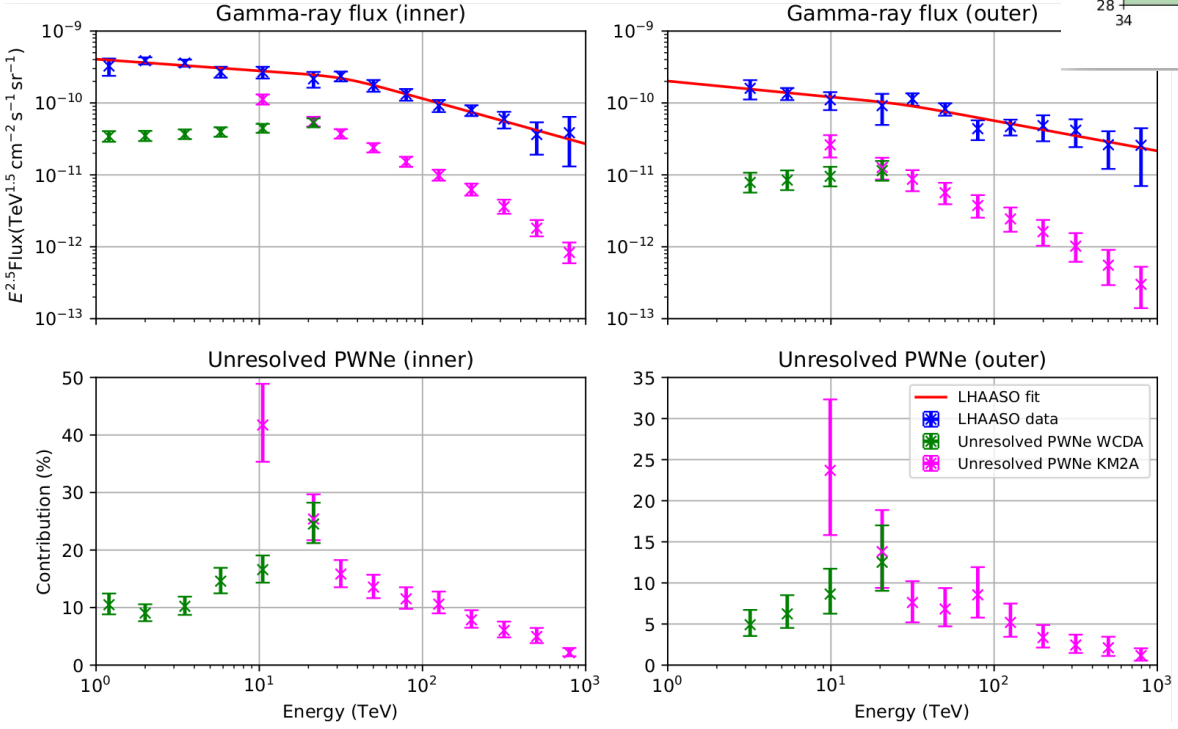

→ The contribution of PWNe to the diffuse background is rather negligible.

→ It peaks at 30% at most at 25TeV in the inner Galaxy.

Diffuse VHE γ-ray emission from discrete sources

SIMULATION:

Kaci & Giacinti, JCAP 01, 049 (2025)

Isotropic and homogeneous diffusion

1) GALPROP-like (d=1/3) :

$$D(E) = 10^{28} D_{28} \left(\frac{R}{3GV}\right)^{\delta} cm^2/s$$

$$D_{28} = 1.33 \times \frac{H}{kpc}$$

2) Time-dependent (mimics self-confinement): 1/100 x D around sources for 10 kyr.

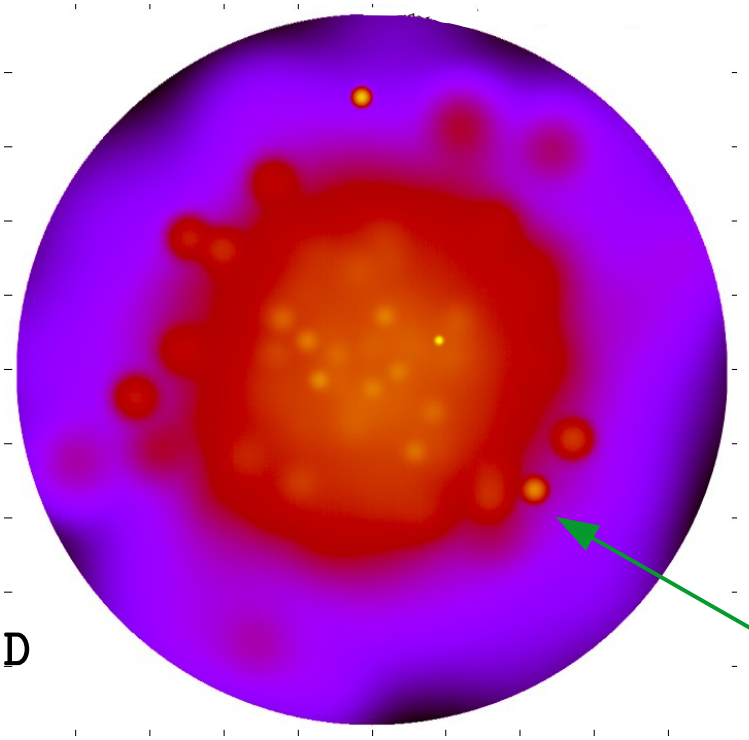

Cosmic-ray flux at Earth and B/C ratio satisfied

Discrete injection of cosmic rays

Clumps in the gamma-ray flux

Kaci & Giacinti, JCAP 01, 049 (2025)

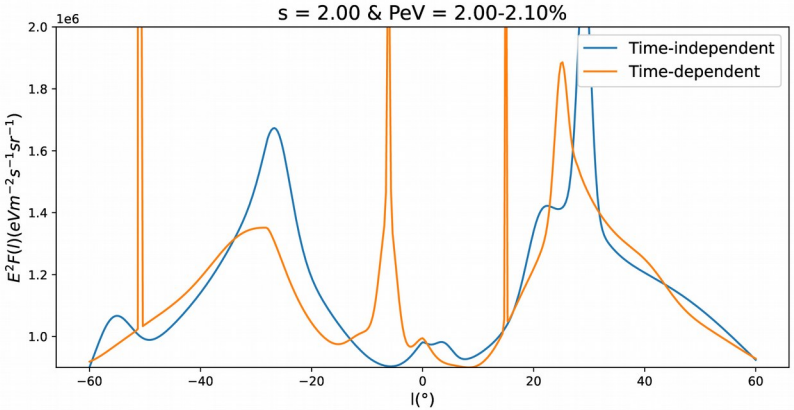

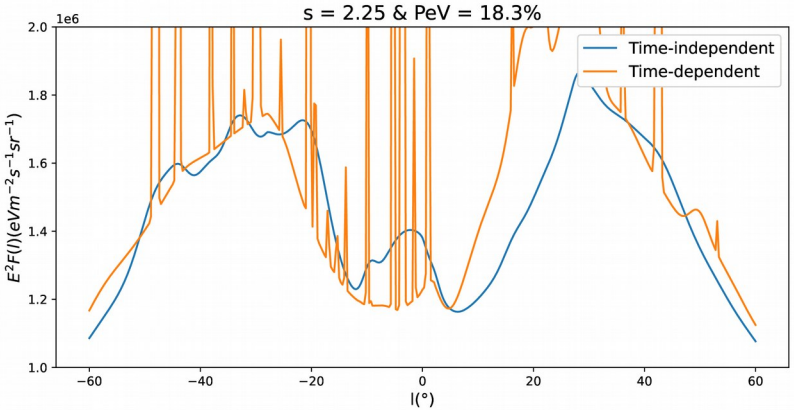

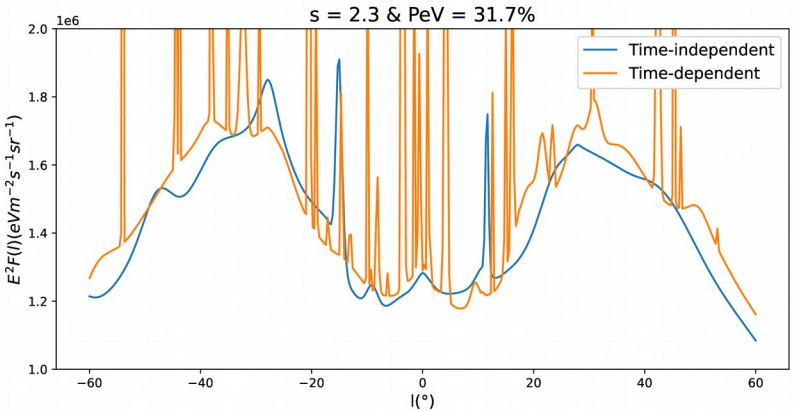

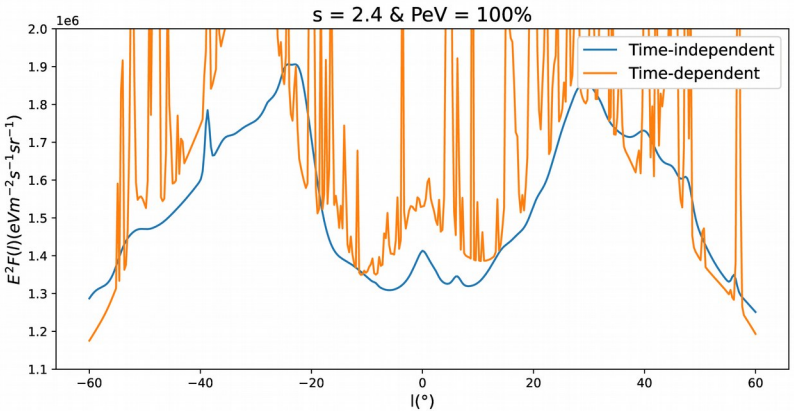

Vs shape from Lipari & Vernetto(2018):

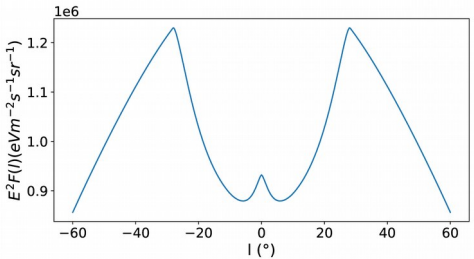

Diffuse gamma-ray flux clumpy at VHE

Sky Maps and sources (case 1)

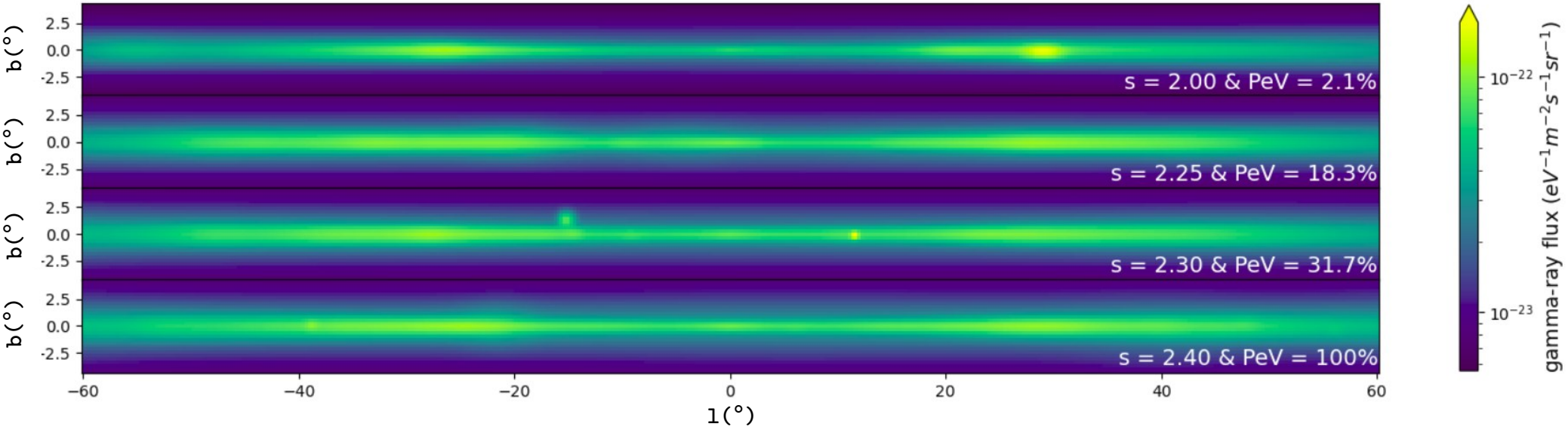

Very few visible sources for case 1

For standard isotropic diffusion, few PeVatrons are detectable

Slide from Samy Kaci

Kaci & Giacinti, JCAP 01, 049 (2025)

Sky Maps and sources (case 2)

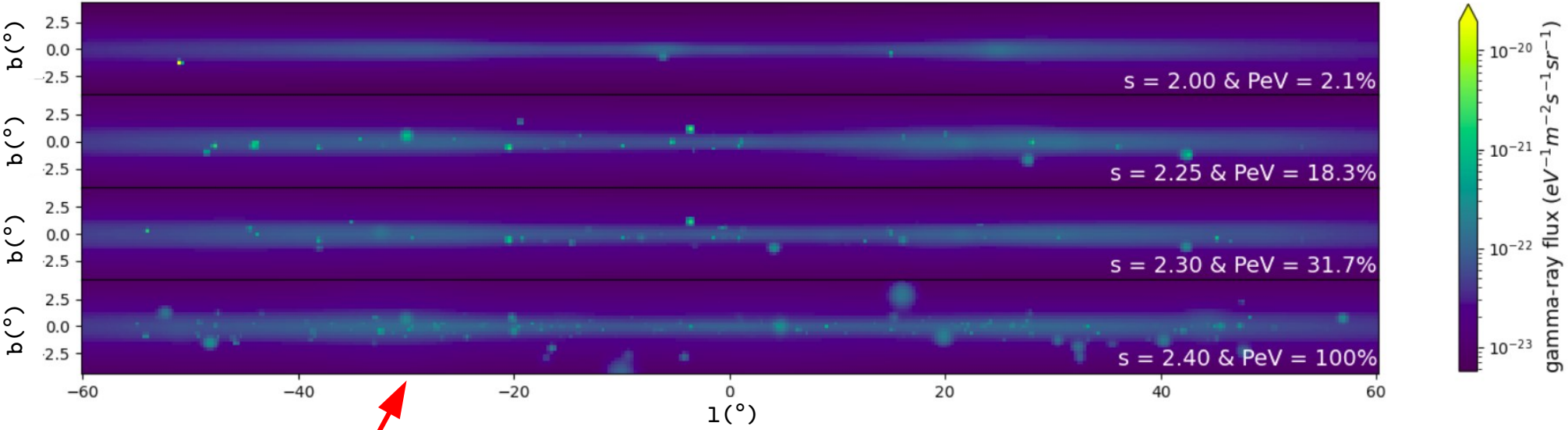

Sky map very sensitive to CR propagation assumptions

Many more visible sources

Implies a PeVatron SNR rate < 3.6/kyr

Slide from Samy Kaci

Kaci & Giacinti, JCAP 01, 049 (2025)

Number of detectable sources

Kaci & Giacinti, JCAP 01, 049 (2025)

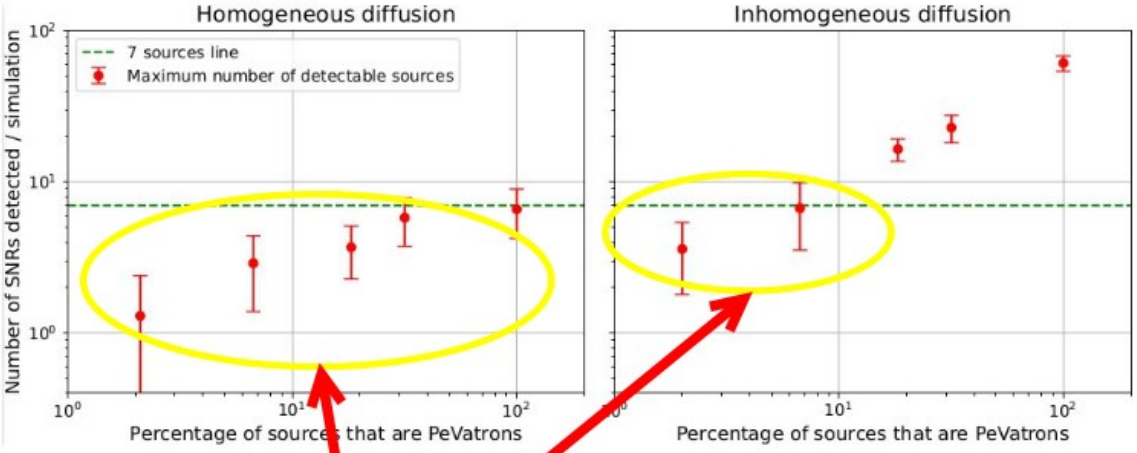

There is still some degeneracy between the two cases

Can be disentangled from clumpiness of diffuse bkg

- Two diffusion regimes lead to different results concerning the detectability of sources.
- Homogeneous diffusion strongly limits the detectability of sources.
- Some parts of the space paramters can already be excluded.

Z. Cao et al., (2023)

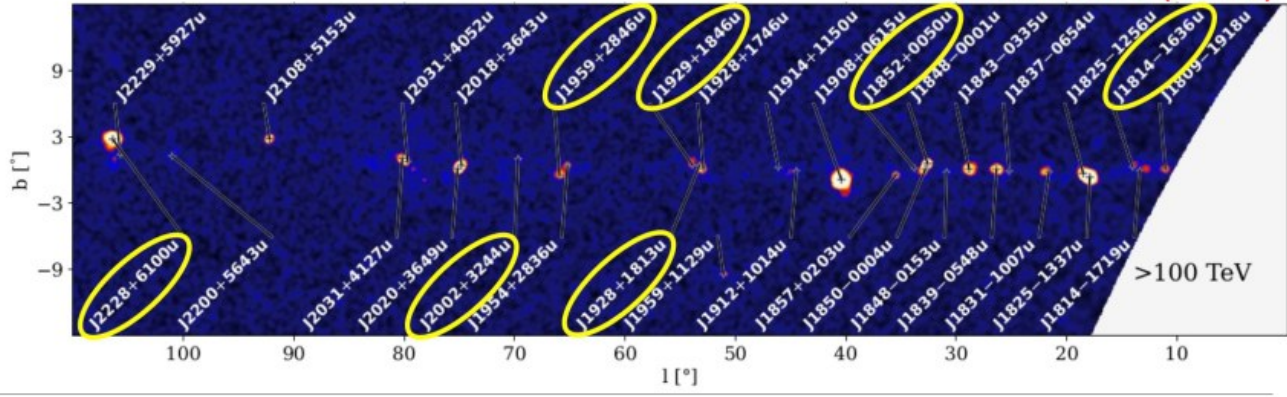

Microquasars as Galactic super-PeVatrons

Kaci, Giacinti, Aharonian & Wang, Submitted to PRL

Microquasars: inj. -2 spectrum, cutoff at 10 PeV, 100 kyr lifetime, 0.1/kyr rate, power $10^{39\text{-}40}$ erg/s.

(Standard/SNR sources: -2.7 Power-law & exponential cutoff at ~ 150 TeV.)

→ **Fits the ~ 10TeV bump, ~ 100 TeV hardening and the knee**

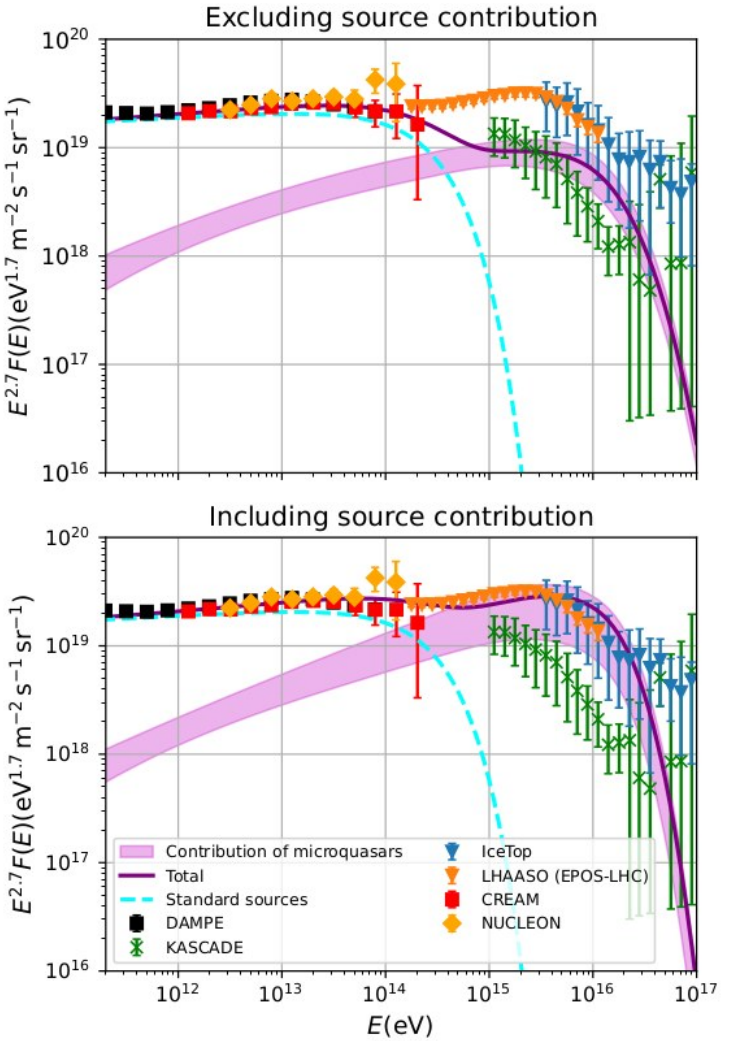

Microquasars as Galactic super-PeVatrons

Kaci, Giacinti, Aharonian & Wang, Submitted to PRL

On average 3-4 sources detectable:

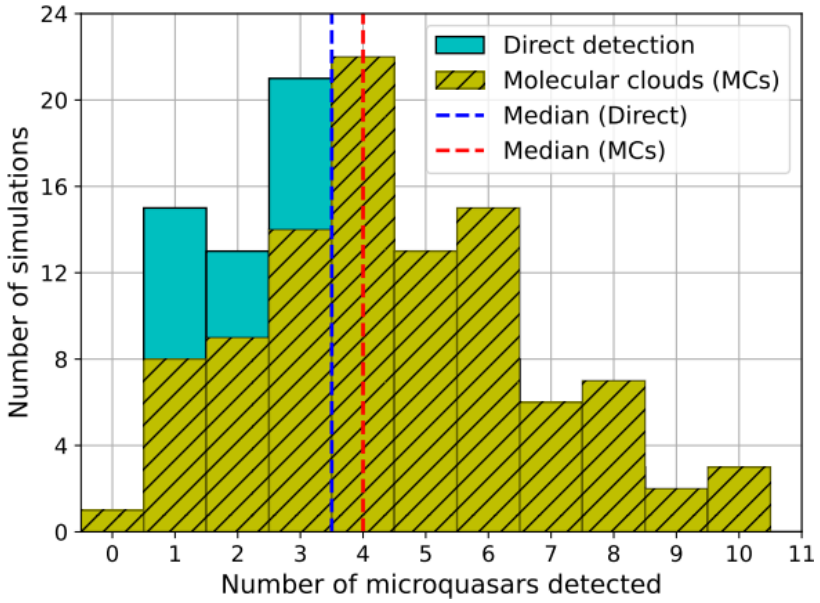

molecular clouds similar to that around SS433
(uniform sphere with r = 20pc and n=30cm^{-3})

Contribution to the diffuse emission:

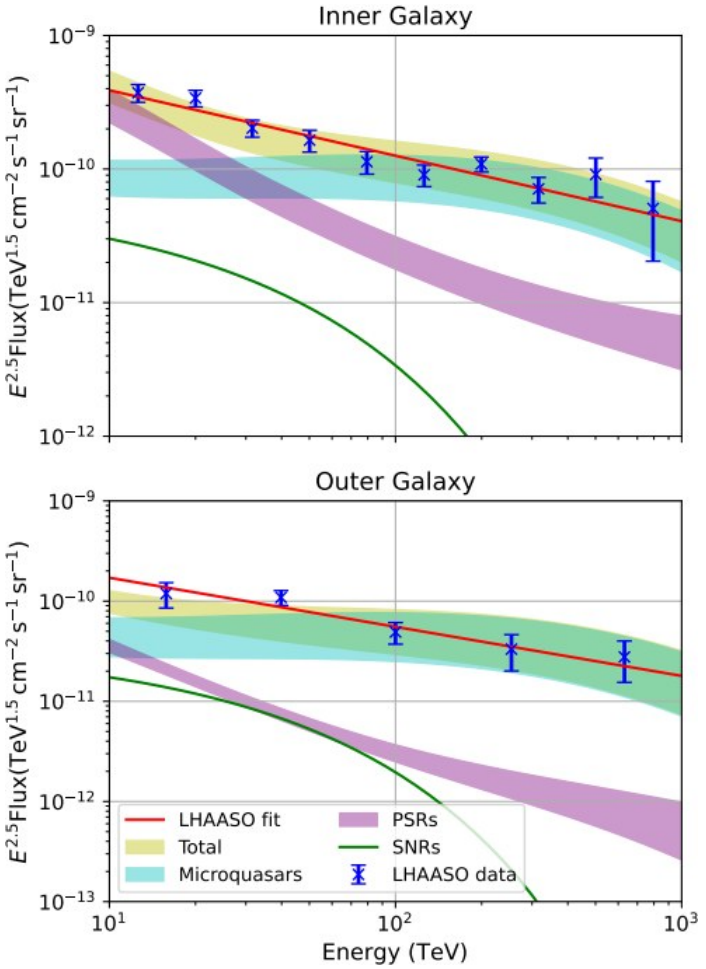

3 – Microquasars

LHAASO's PeVatron microquasars

LHAASO Collaboration, National Science Review (2025)

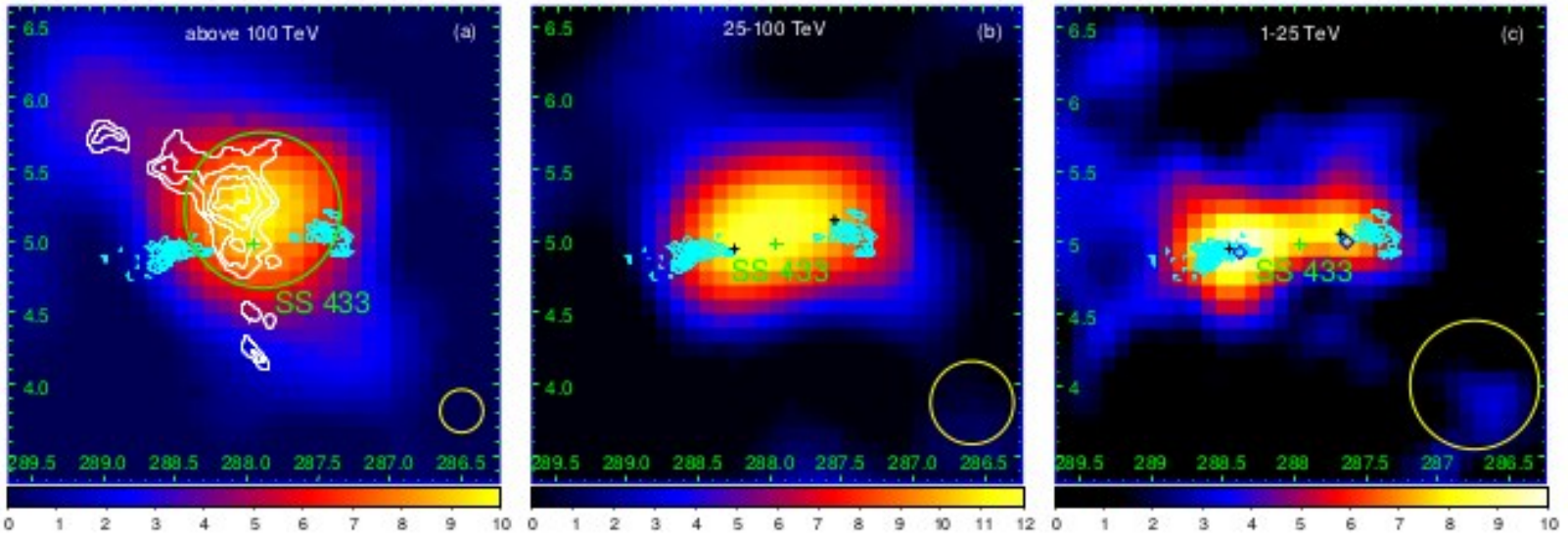

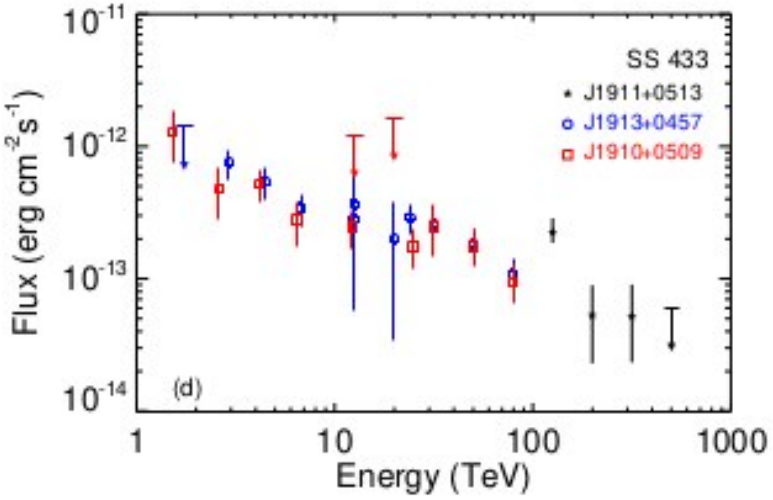

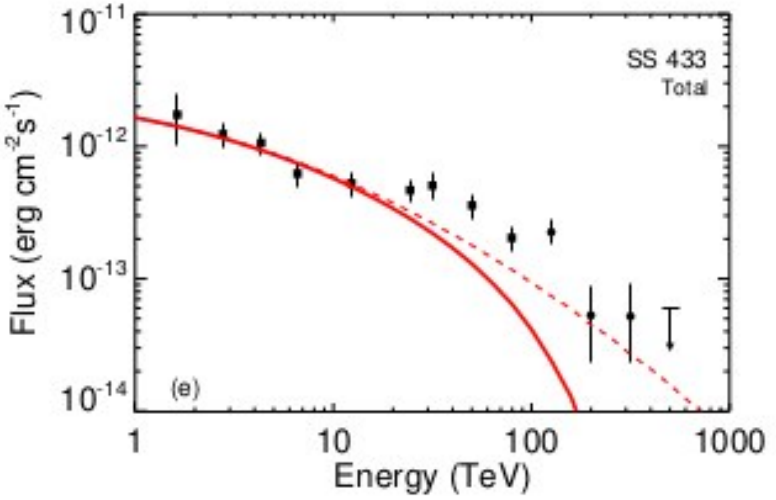

LHAASO's PeVatron microquasars

LHAASO Collaboration, National Science Review (2025)

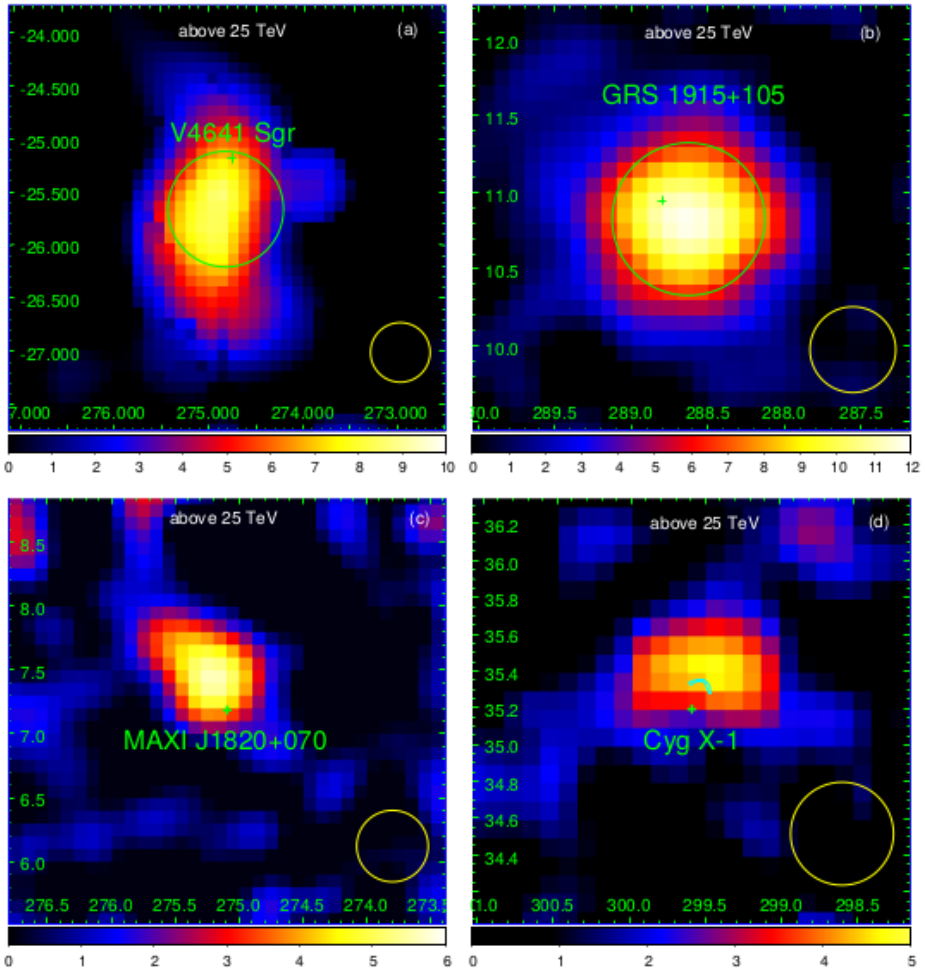

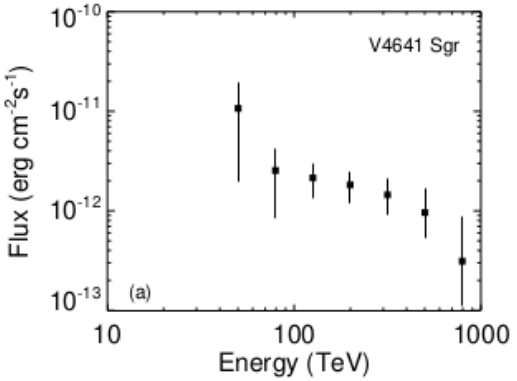

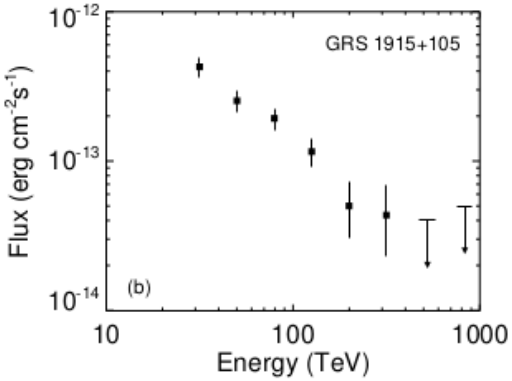

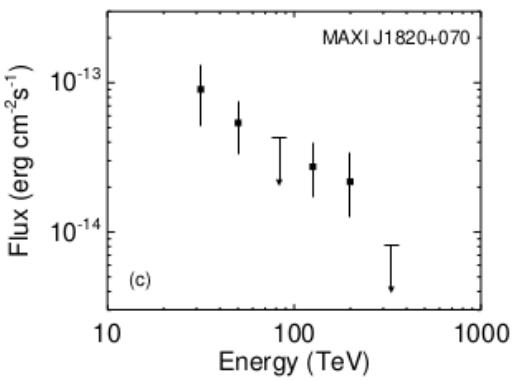

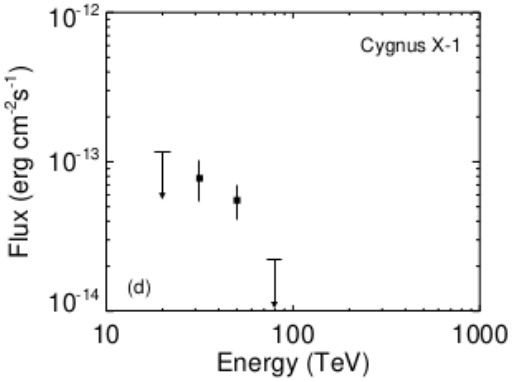

Acceleration mechanism?

RESEARCH

GAMMA-RAY ASTRONOMY

Acceleration and transport of relativistic electrons in the jets of the microquasar SS 433

H.E.S.S. Collaboration*†

H.E.S.S. Collaboration,
Science **383**, 402–406 (2024)

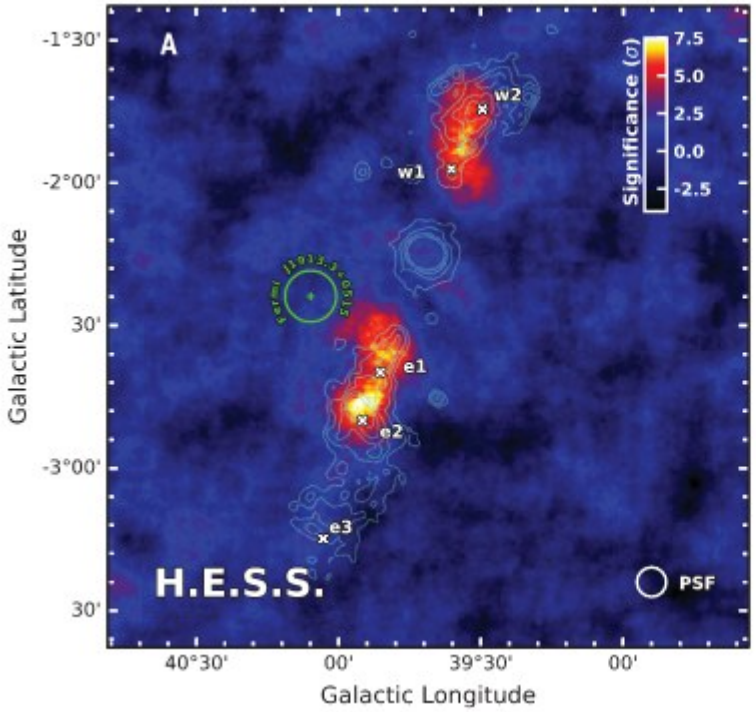

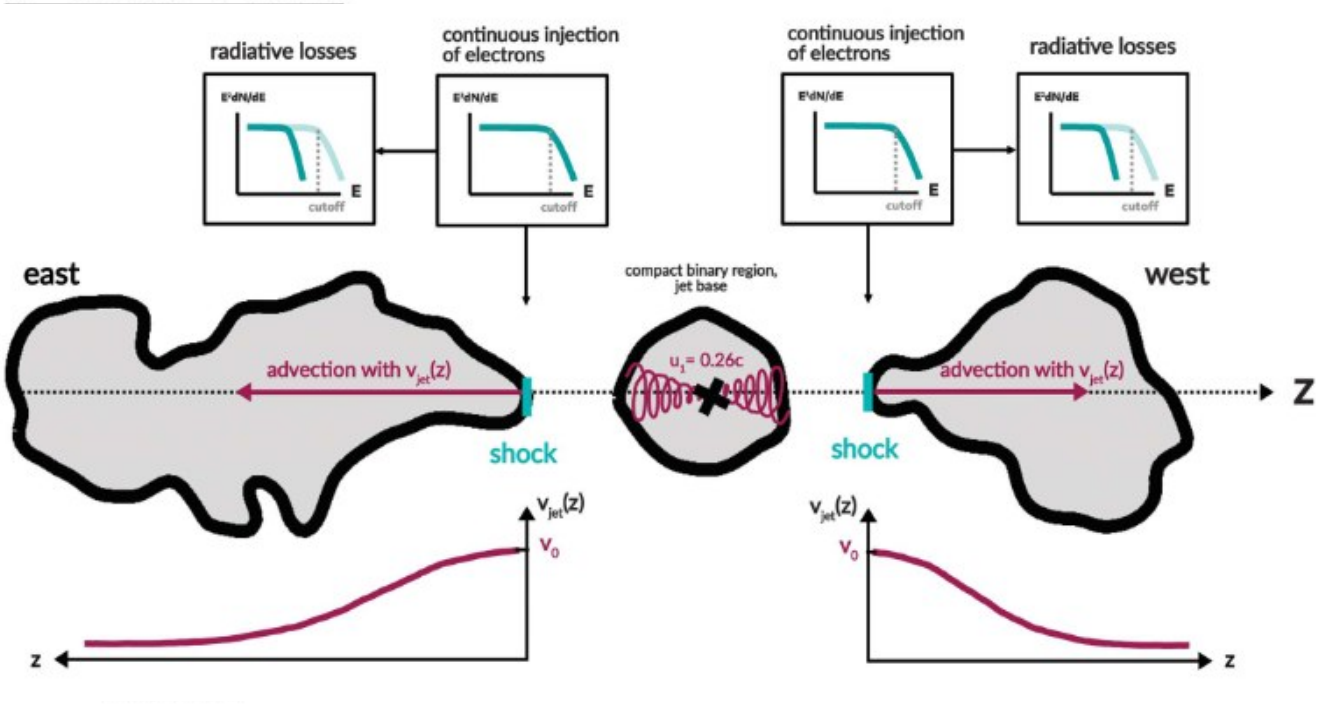

In-situ particle acceleration, to > 100 TeV.

Particle-In-Cell (PIC) simulations

→ **Unmagnetized case** (σ=0):

Spitkovsky (2008), Sironi + (2013), Plotnikov+ (2018), Lemoine+ (2019)

Relativistic unmagnetized shocks
Good but slow accelerators.

Maximum energy grows as $t^{1/2}$
(Reville & Kirk 2010, Plotnikov et al. 2013)

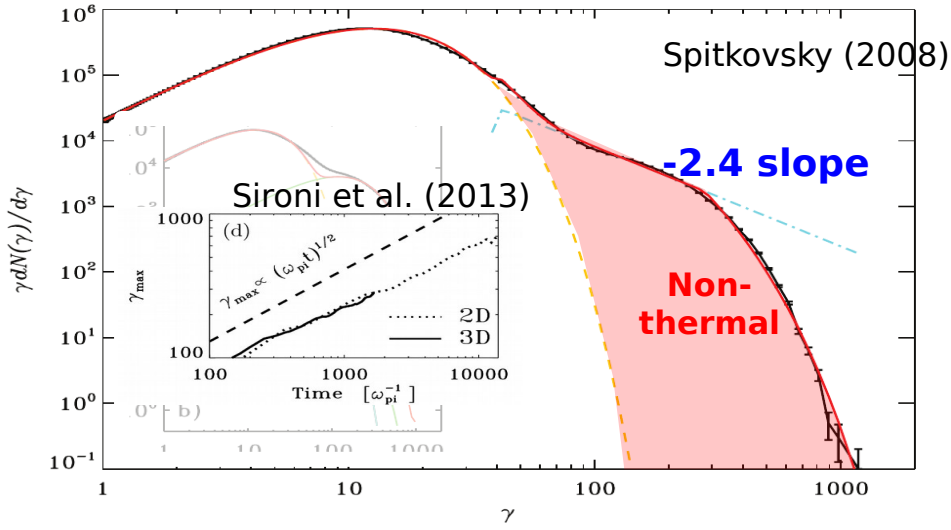

→ **Magnetized case** ($\sigma>10^{-3}$):

Even weak magnetization levels stop particle acceleration.

E_{max} quickly saturates.

Cannot accelerate to VHE!

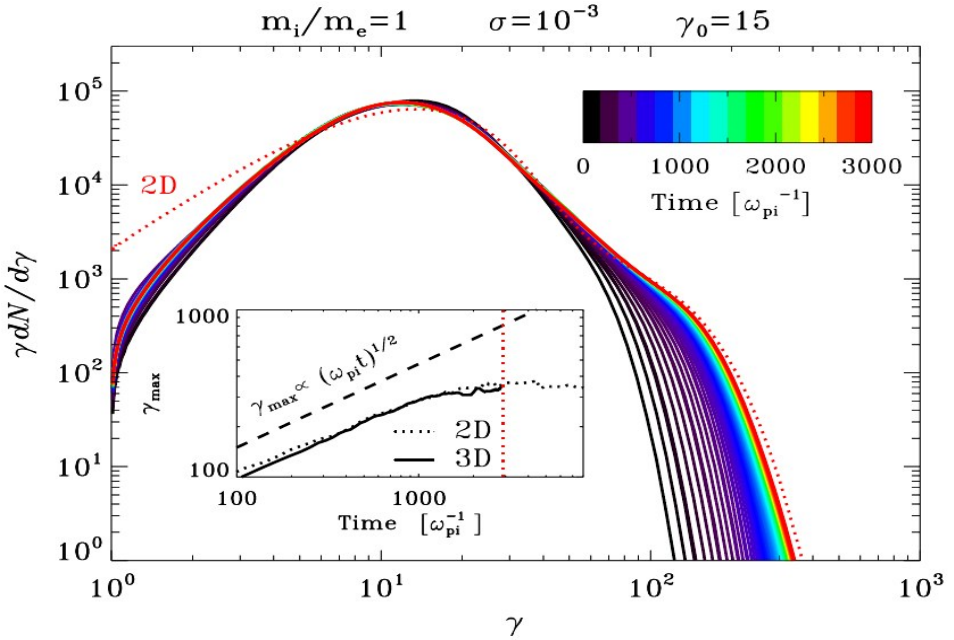

Sironi et al. (2013)

Solution: Global B field geometry

LARGE-SCALE GEOMETRY OF THE B FIELD MAY SOLVE THE PROBLEM!

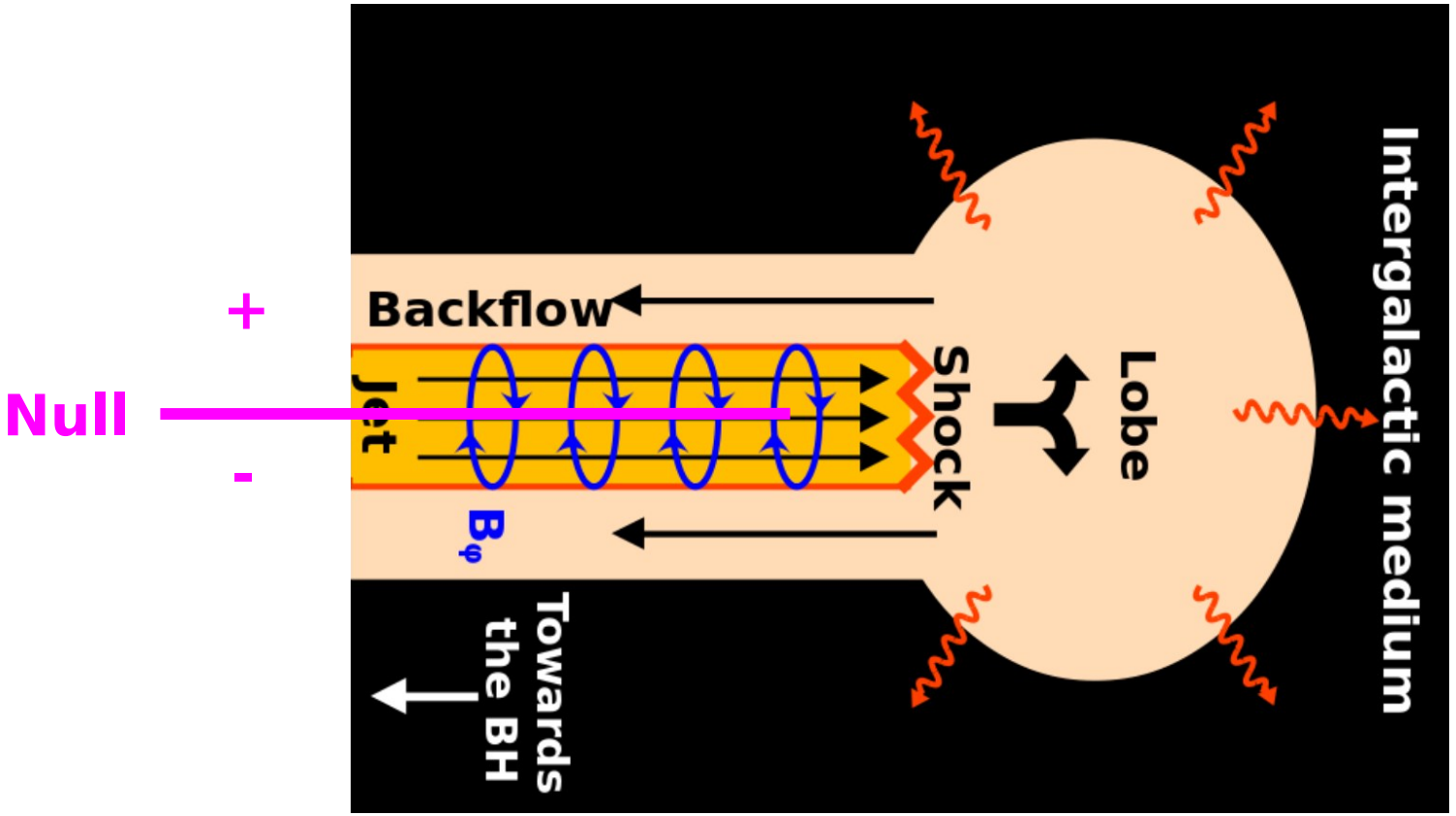

Cerutti & Giacinti, A&A (2023)

Numerical simulations

POSITRONS:

ELECTRONS:

(roles exchanged with opposite pulsar polarity)

No/little acceleration

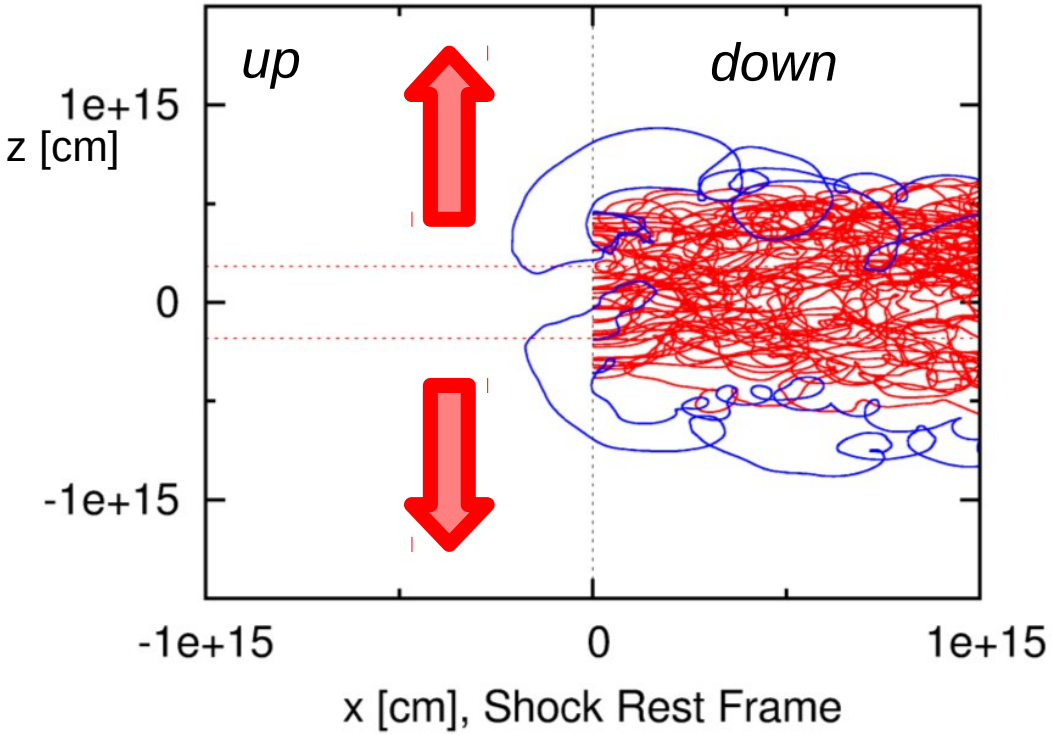

Efficient acceleration to VHE !

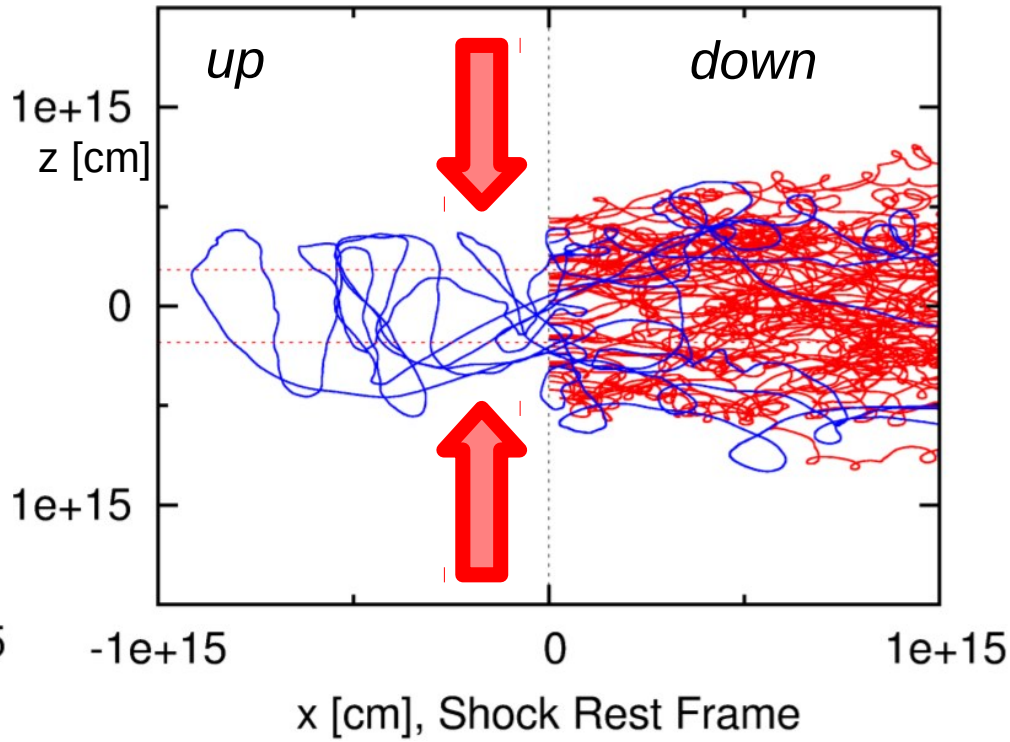

GG & Kirk, ApJ **863**, 18 (2018)

Cerutti & Giacinti, A&A **642**, A123 (2020); A&A **656**, A91 (2021)

Results PIC : Density evolution

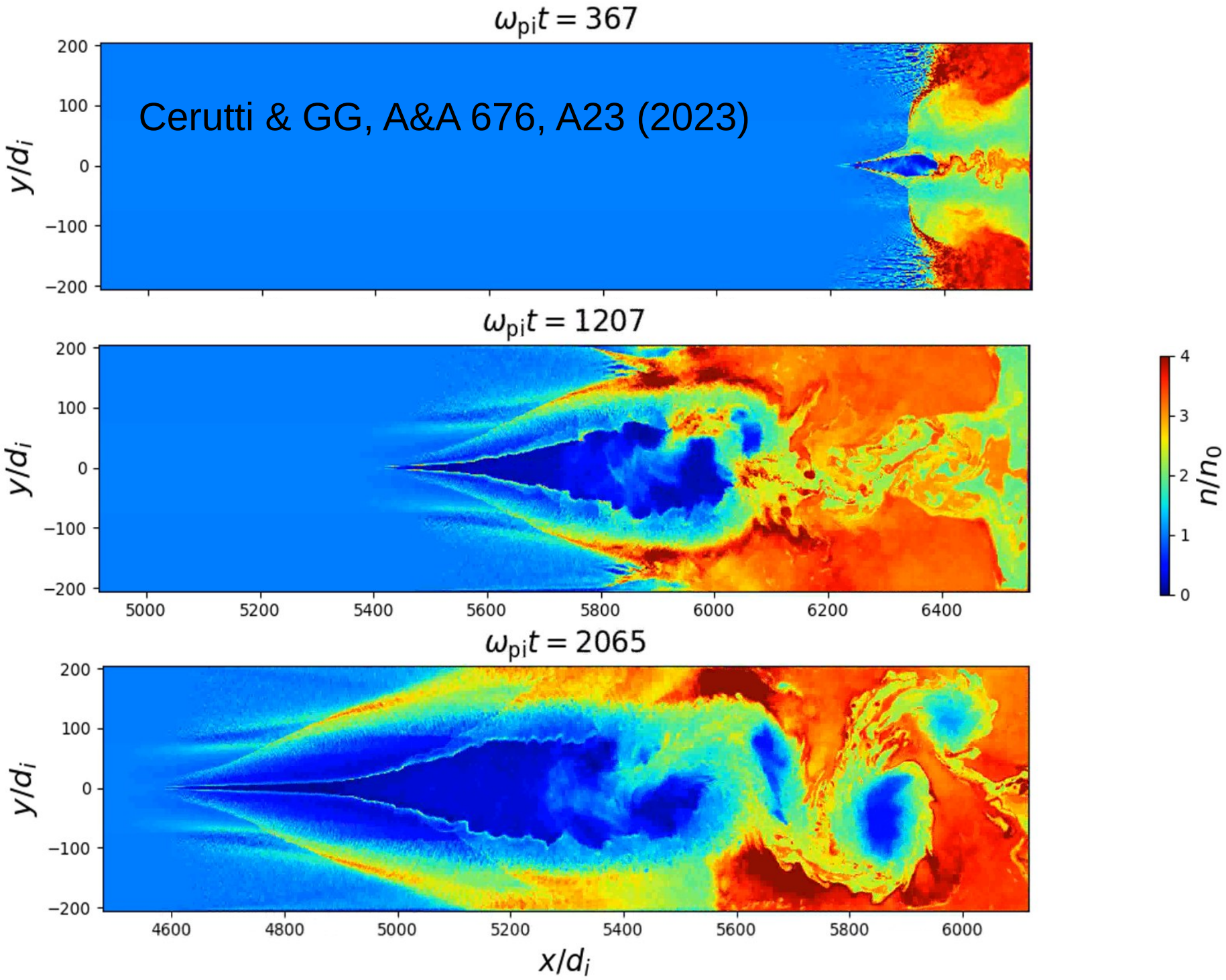

Particle-In-Cell (PIC) setup

2D Cartesian box (xz-plane), **262,144×16,384 cells, or 6554x410 d_i (ion skin depth)**

Electron-ion plasma with **m_i/m_e=25**

Magnetization : **σ=0.1, 1**

Reflecting boundary
= contact discontinuity

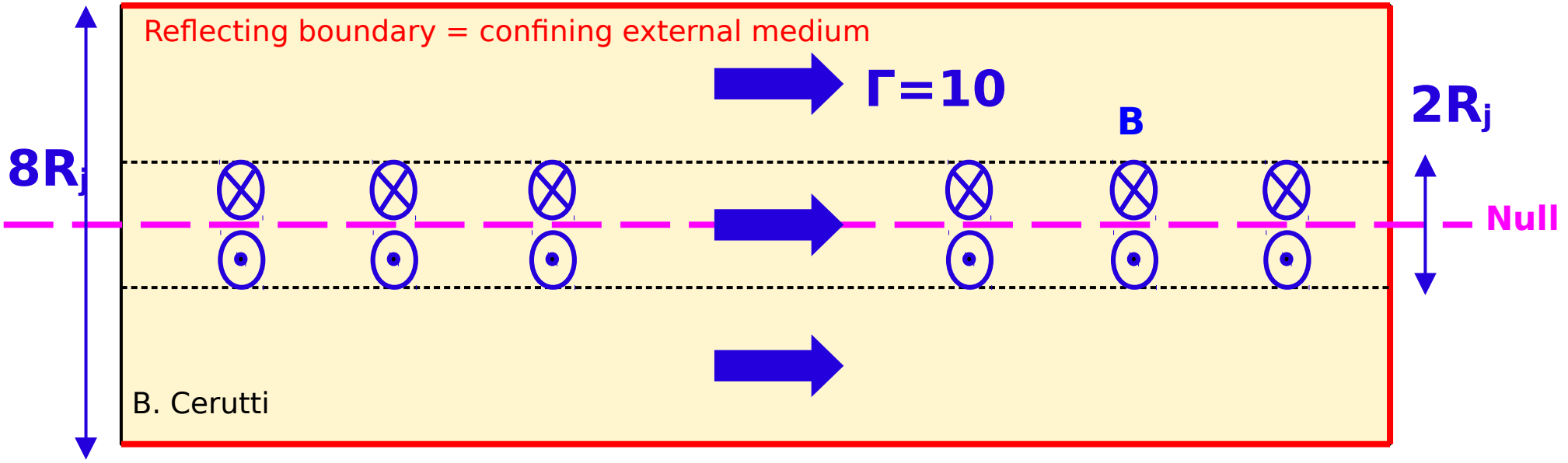

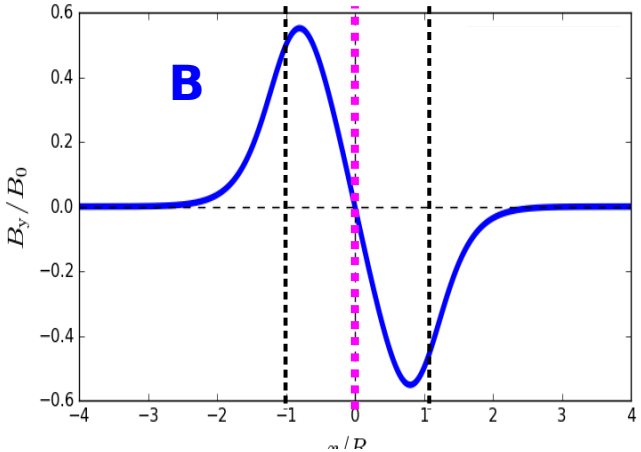

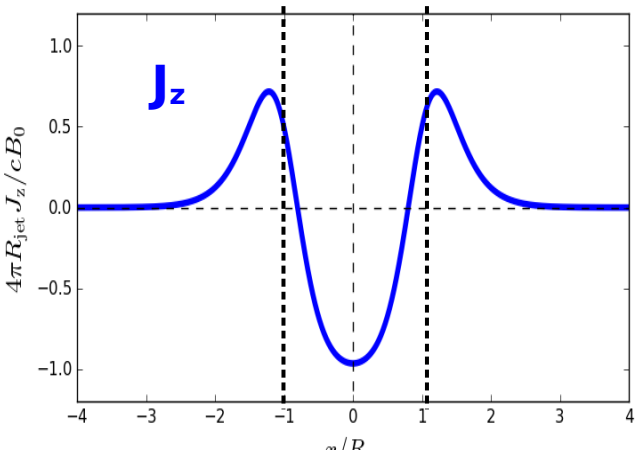

Results – PIC Simulations

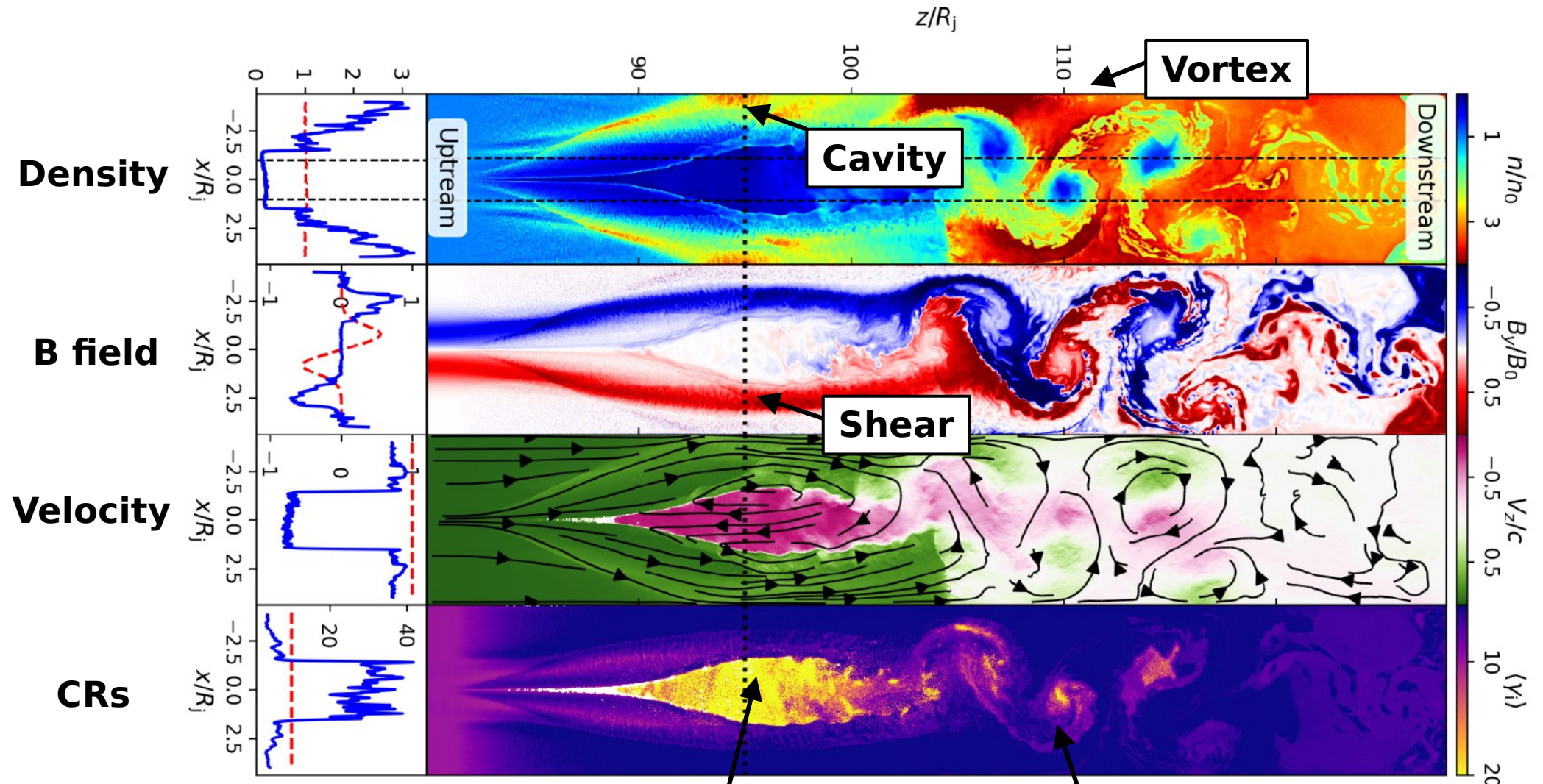

Cerutti & GG, A&A 676, A23 (2023)

HE particle <u>acceleration</u>

HE particle <u>escape</u>

→ Shear-flow acceleration at the edges of the cavity

Ion spectrum: Time Evolution & E_{max}

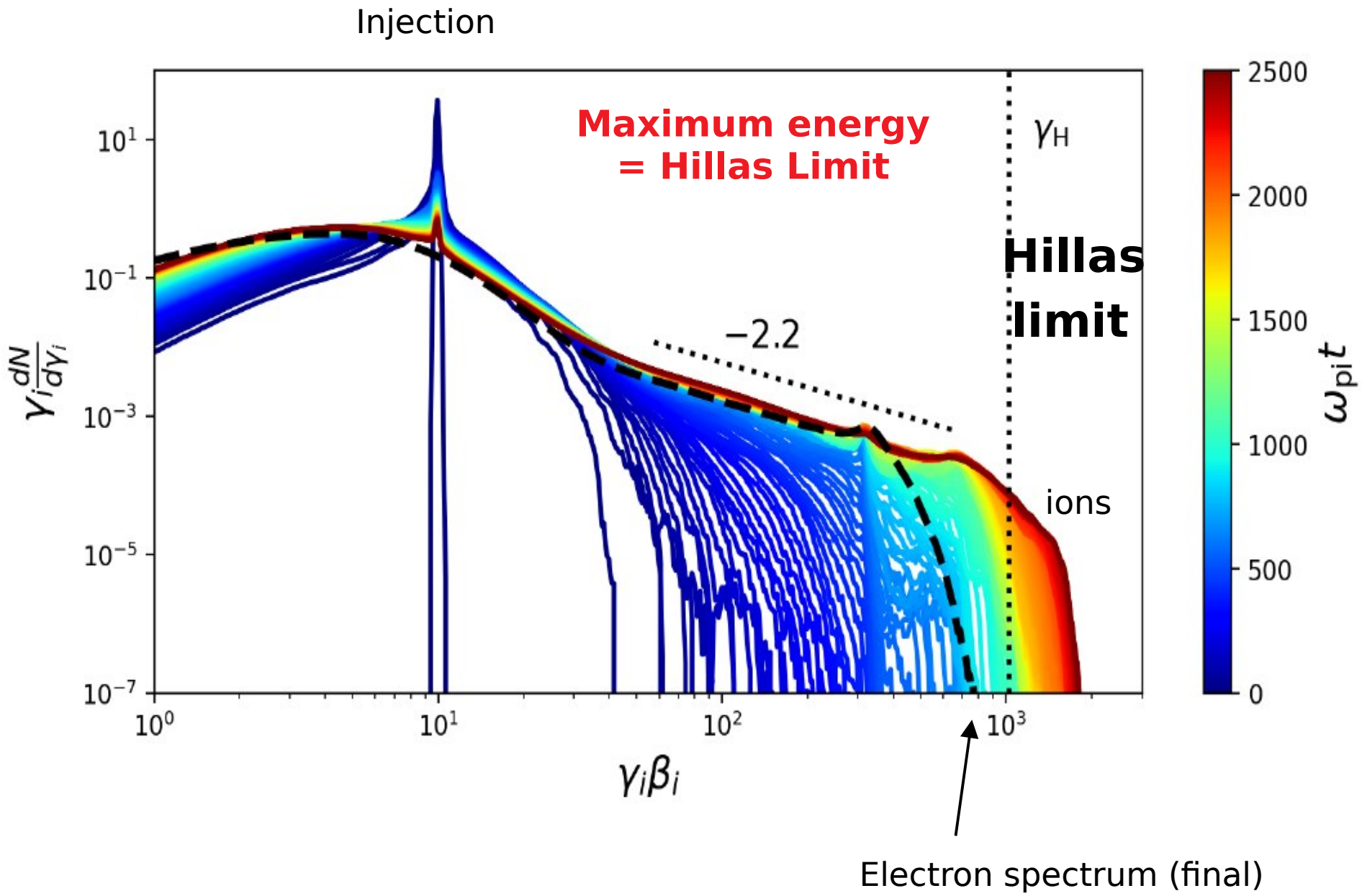

4 – CR anisotropy

Bian, Giacinti & Reville, ApJ 979, 197 (2025)

HAWC + IceCube Collab., ApJ (2018) [arXiv:1812.05682]:

Large Scale Anisotropy (~0.1%) :

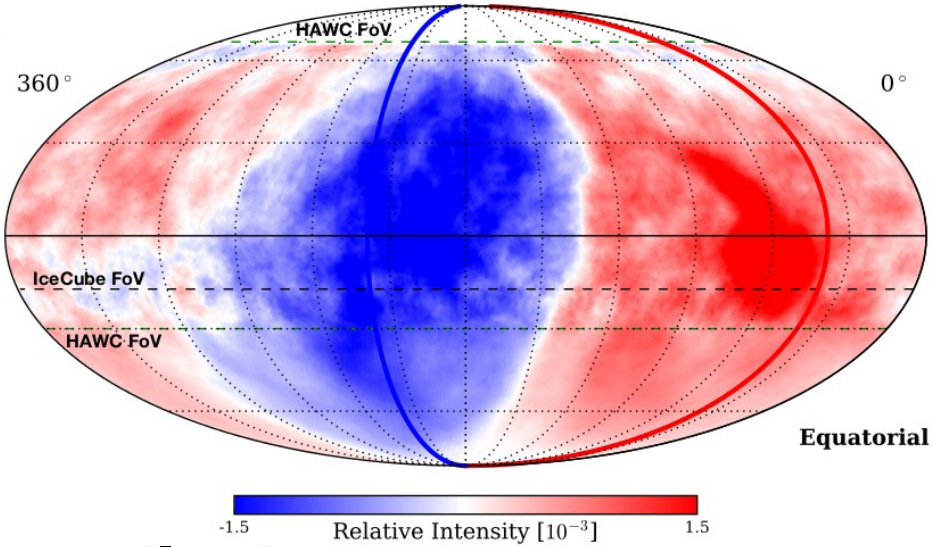

In the direction of field line

SSA (I>3):

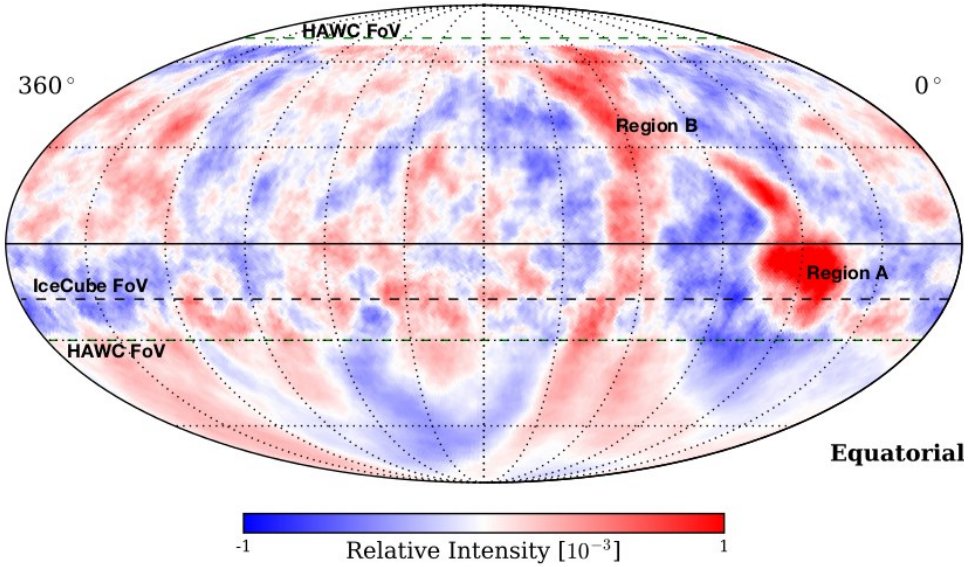

Angular power spectrum:

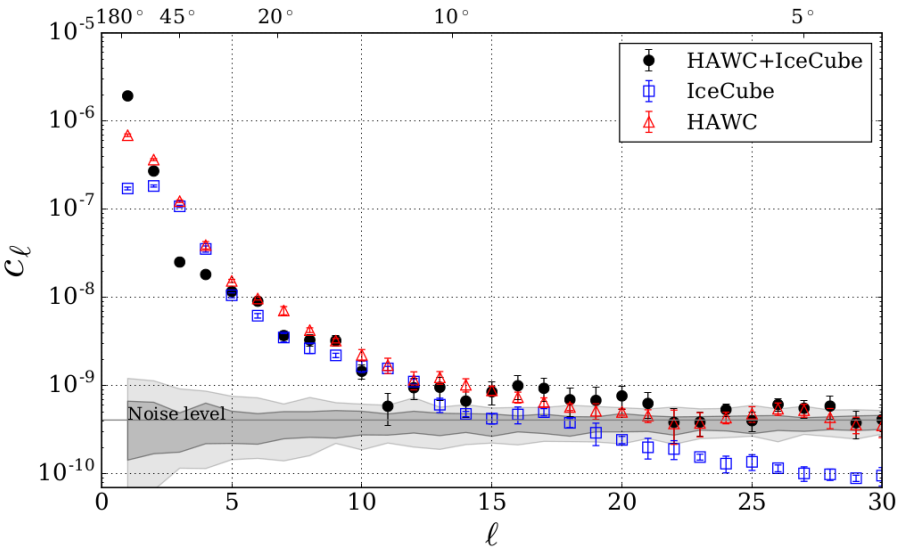

Small-scale anisotropies

Giacinti & Sigl, Phys. Rev. Lett. (2012), arXiv:1111.2536

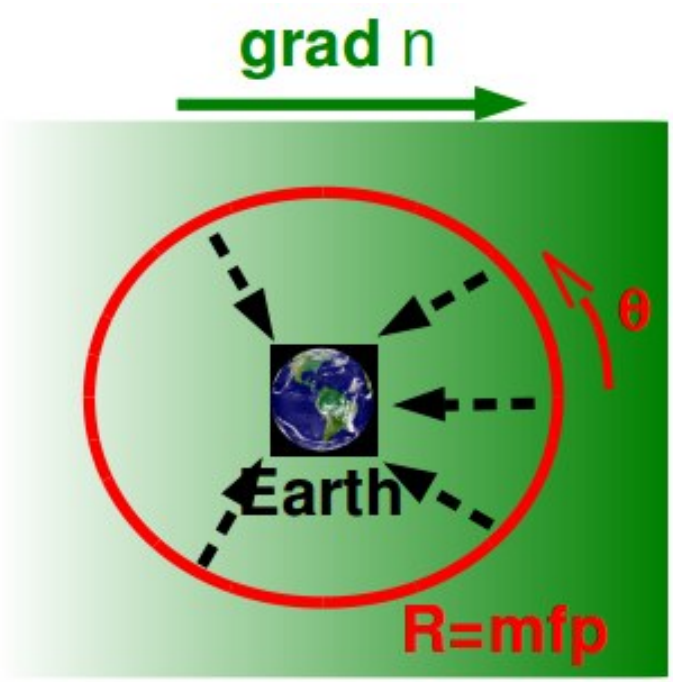

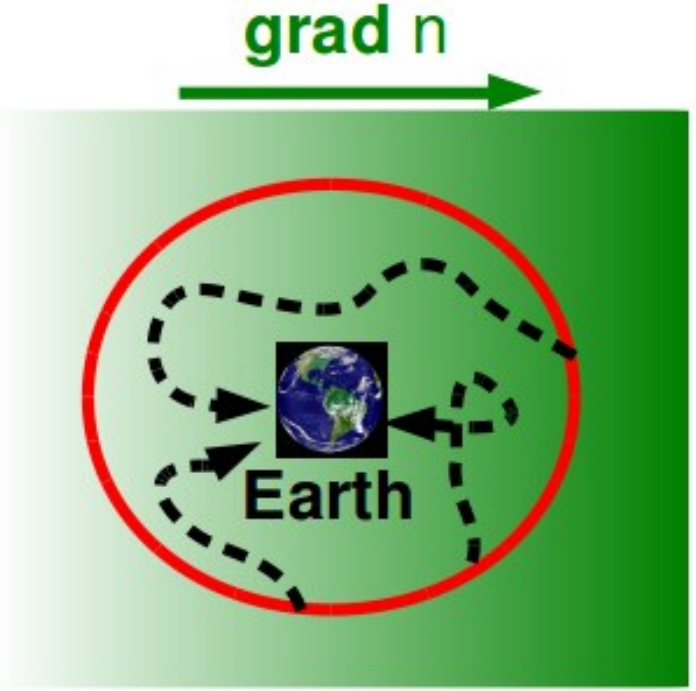

$$F = F_0 (1 + \delta \cos \theta)$$

SSA due to the local realization of the ISM turbulent field, within a CR MFP around Earth.

CR anisotropy down to 3 TeV

Bian, Giacinti & Reville, ApJ (2025)

Simulations now reach TeV energies

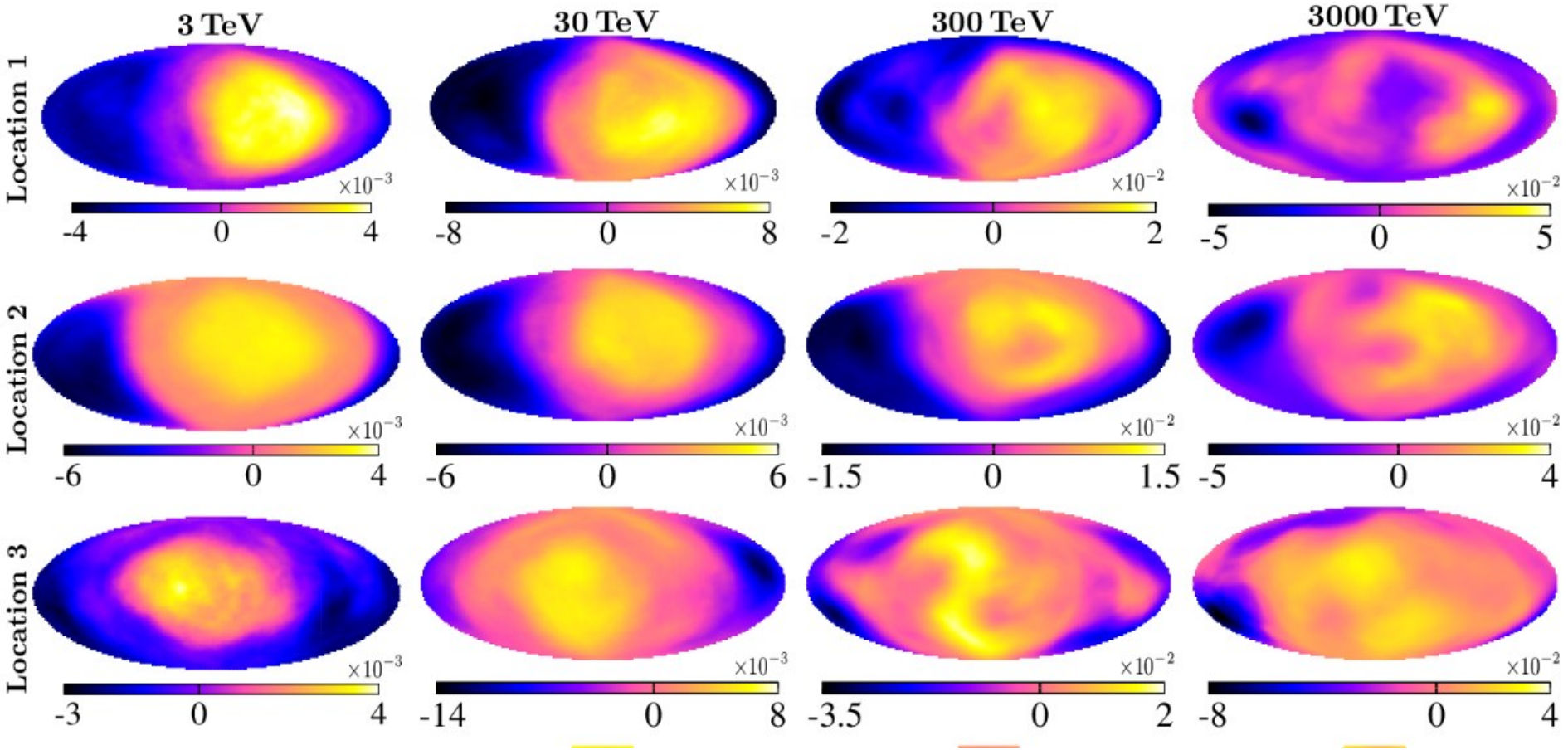

Outer scale turbulence L_{max} = 150 pc, Kolmogorov turbulence

CR anisotropy down to 3 TeV

Bian, Giacinti & Reville, ApJ (2025)

Simulations now reach TeV energies

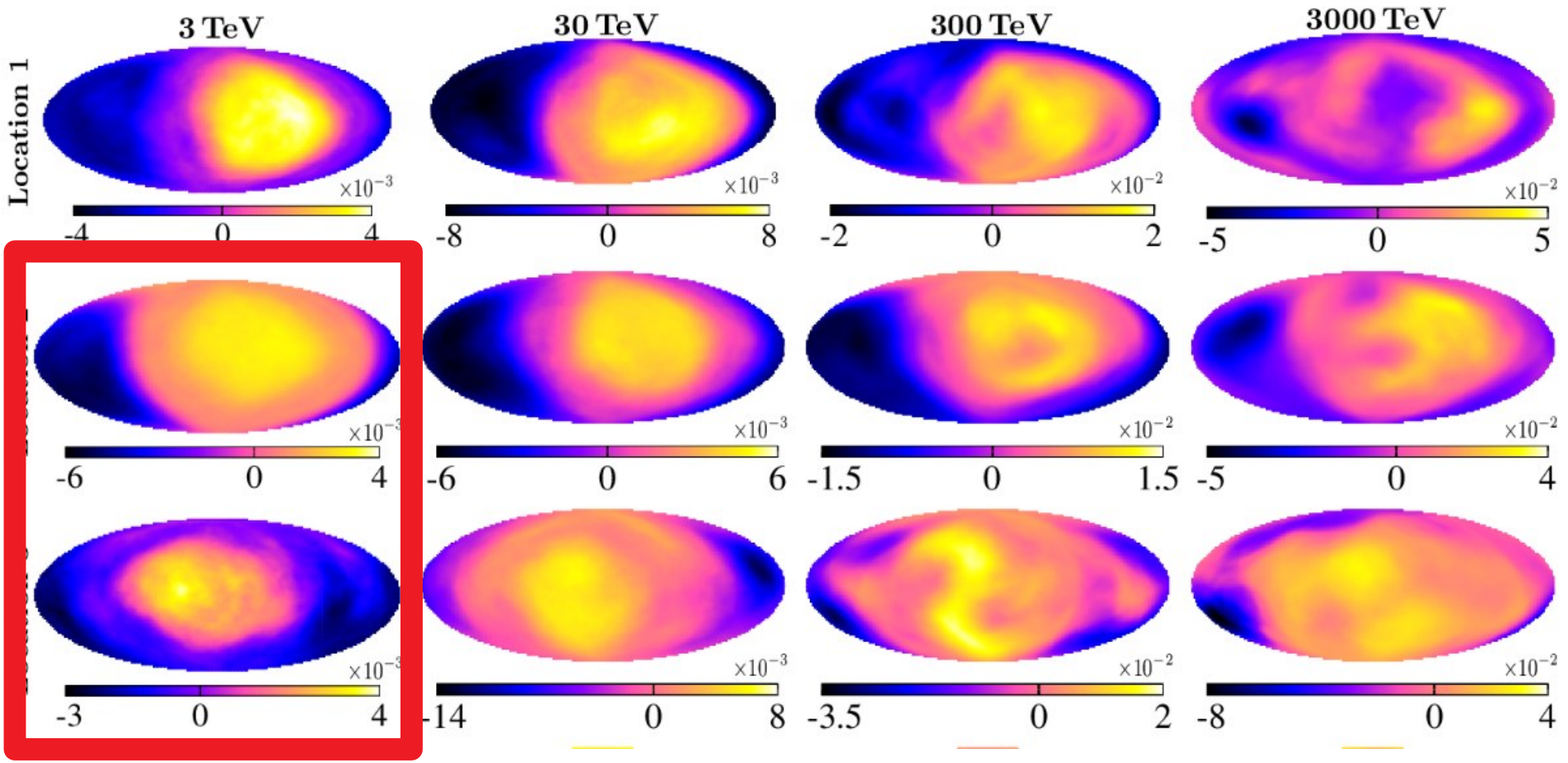

Amplitude SSA/LSA related to local

Power spectrum versus CR energy

Spherical harmonics: $$f(E,\mu,\phi) = \sum_{\ell=0}^{L_{max}} \sum_{m=-\ell}^{\ell} f_\ell^m(E) Y_\ell^m(\mu,\phi)$$

Angular power spectrum: $$C_\ell = \frac{1}{2\ell+1} \sum_{m=-\ell}^{\ell} |f_\ell^m|^2$$

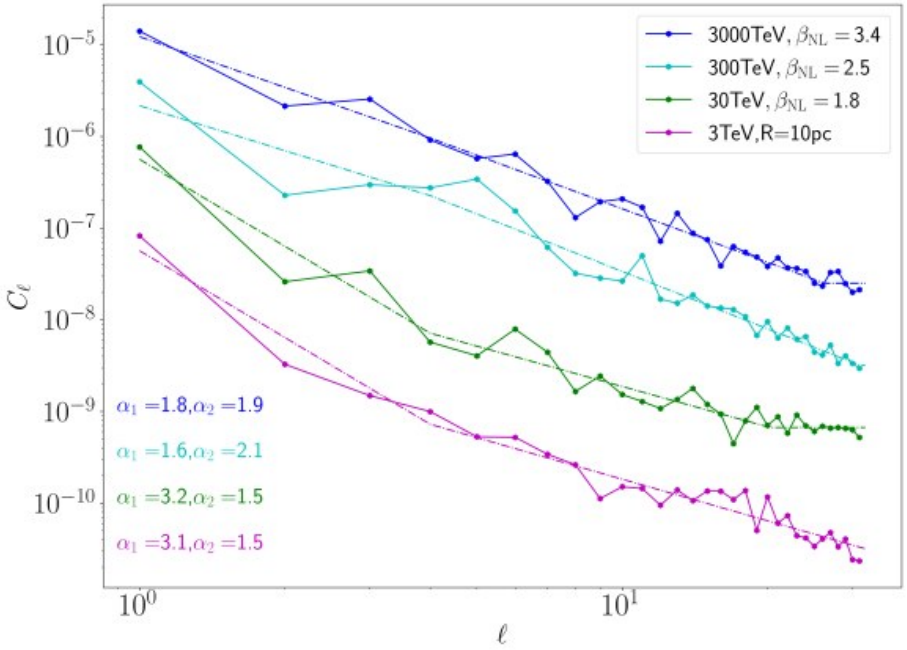

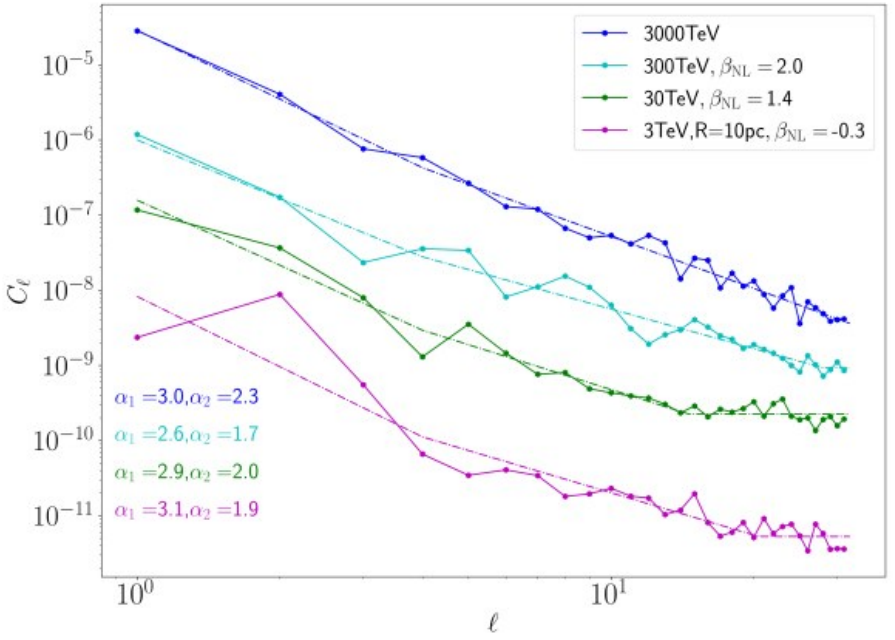

Power spectrum versus CR energy

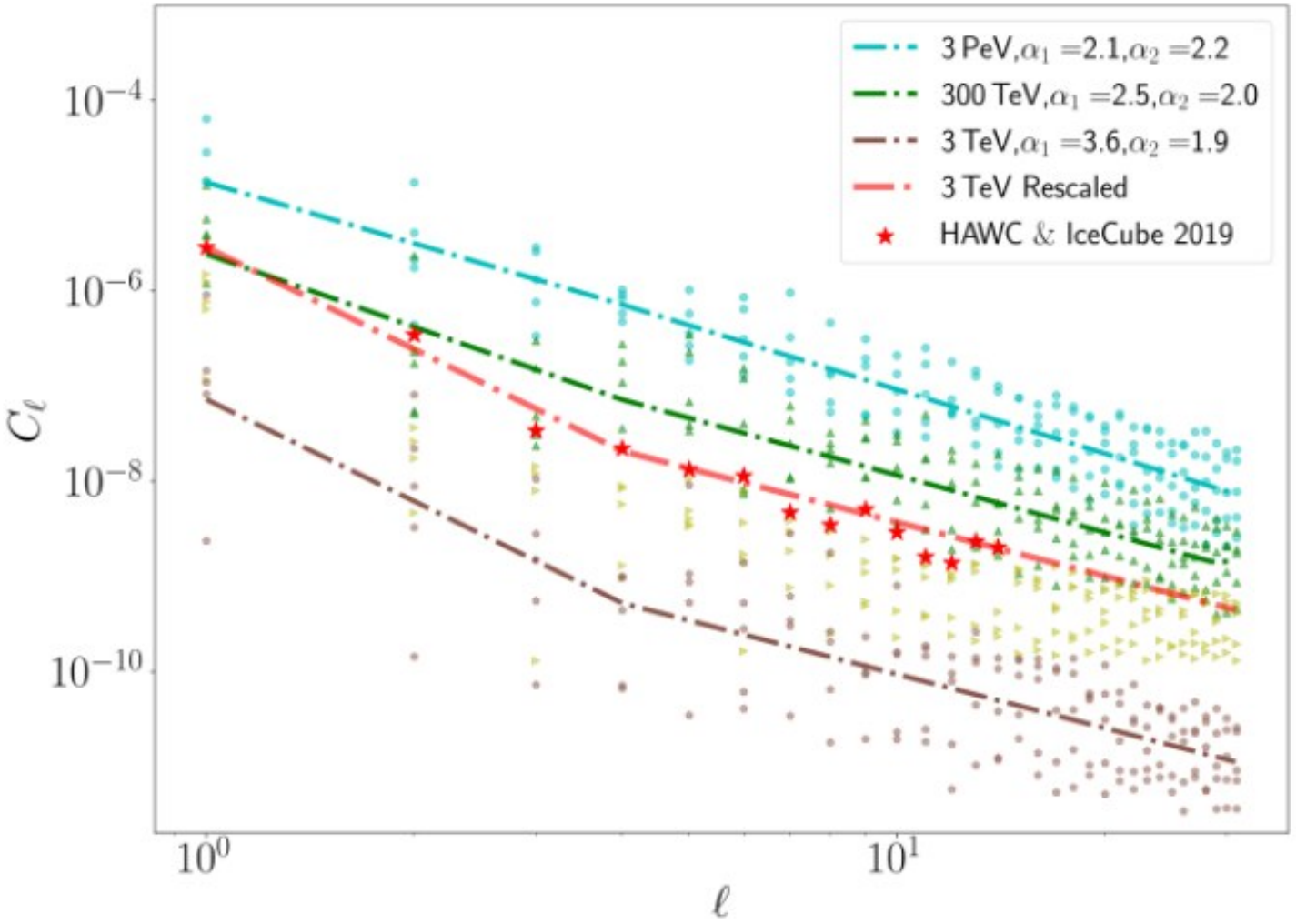

Excellent agreement with HAWC & IceCube measurements

Conclusions & Perspectives

→ **TeV halos** constrain CR propagation around middle-aged pulsars,

→ **Best fit** parameters for **Geminga.** Inner asymmetries can help disentangle between Kolmogorov (slightly favored) and Bohm,

→ **“Mirage” sources, asymmetric γ-ray sources**: **Could explain some LHAASO sources,**

→ **Clumpy diffuse γ-ray background at VHE,**

→ **Unresolved PWNe/halos**: Minor contribution to LHAASO diffuse emission at > a few 10 TeV,

→ Observations not incompatible with frequent transient PeVatrons with standard CR diffusion coefficient,

→ ~ 10 powerful **microquasars can fit CR spectrum and LHAASO diffuse γ-ray emission.**

→ **TeV-PeV CR anisotropy angular power-spectrum** can constrain interstellar turbulence properties.